

4 DIE-PLUNGER COMPRESSION TEST

4.1 Experimental methods

One aim of this research work was to establish a correlation between the stability of graft materials against stem subsidence in impaction grafting, which is a complex loading situation, and fundamental mechanical properties, which are relatively easy to determine and reproduce. A die-plunger compression test was used to measure basic properties like compression stiffness, relaxation and elastic recoil. These properties influence mechanical stability against subsidence in impaction grafting, the compaction properties and the sensory feedback experienced by a surgeon during impaction.

A simple easily reproducible experiment for quasi-static compression testing was designed using a die and plunger compression device which is commonly used in ceramics laboratories testing. The die-plunger device is normally used to press ceramic powder tablets prior to sintering. The only change required was the reproduction of a matching hollow plunger capped by a porous disk to allow liquid penetration when wet and bloody grafts were tested instead of dry ceramic powders.

The standard die-plunger consisted of a hollow cylinder as a die measuring 80mm in height with polished bore hole of 20mm diameter. The bottom of the die was closed with a 20mm diameter disc which could easily be removed after the experiment to retrieve the specimen. The plunger consisted of the original polished cylinder of 20mm diameter and 100mm length when dry ceramics were tested. When wet or bloody bone grafts or bone plus ceramic mixes were tested, the plunger was formed by a hollow cylinder of identical outer dimensions capped by a highly porous brass disk with negligible resistance against liquid penetration. A schematic drawing of the die-plunger set-up can be seen in figure 4.1 (left).

Using a measuring tube, constant individual 10 cm^3 sample volumes of loose, non-compacted bone graft, granular ceramic or mixes thereof were prepared and settled into the tube by light manual shaking or tapping. The sample was then transferred into the die using a wide funnel to allow fast and uniform charging of the die. The plunger was inserted and the sample volume pre-compressed by a static mass $m= 1\text{kg}$ whilst rotating the plunger. With this weight

constant start conditions were ensured by pushing down and levelling out fatty bone grafts adhering to the die wall or dry ceramics forming uneven top surfaces. The static weight was removed and the start sample height measured with a ruler. The sample volume of $V=10\text{ cm}^3$ converts to a theoretically constant start height of $h_{start}=31.83\text{mm}$ but in practice it varied by approximately 10% in both directions because measuring and charging small volumes of relatively large particles and ensuring homogenous mixing throughout the sample introduced such a tolerance level.

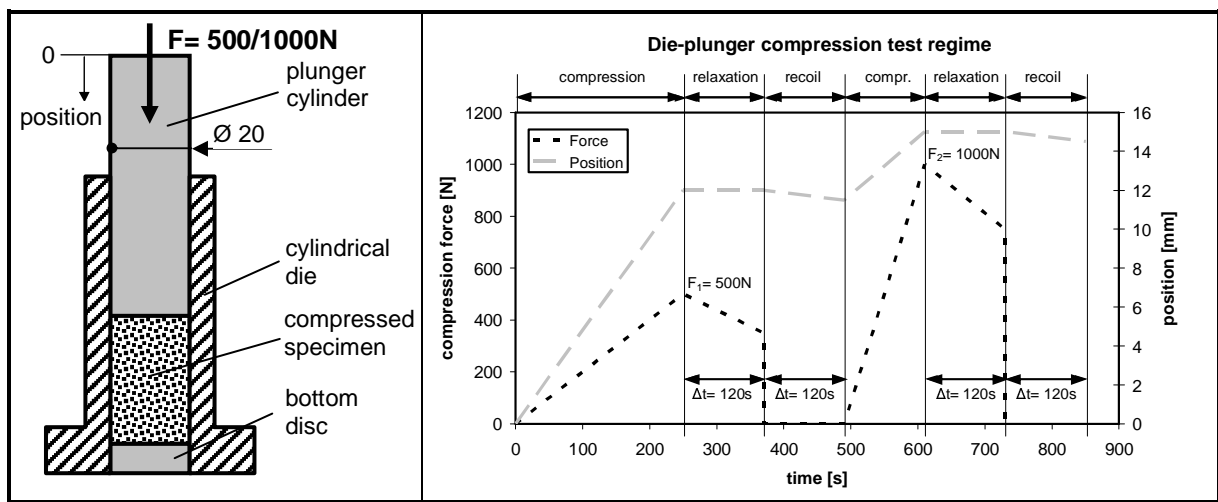


Figure 4.1: Schematic drawing of die-plunger device (left) and chart representing the compression test regime with its two compression, relaxation and recoil phases.

The sample was quasi-statically loaded in compression using a Dartec[®] Series HC10 hydraulic test machine. Crosshead speeds were set at $v_{comp}=2\text{mm/min}$ for ceramics and $v_{comp}=3\text{mm/min}$ for bone grafts and bone/ceramic mixes. Compression force and displacement were measured at an acquisition rate of 5 to 10 points per second with the Dartec “Tool” software. Compression was stopped at a peak force of $F_1=500\text{N}$ which converts to a peak graft stress of $\sigma_{comp}=1.59\text{MPa}$. The sample was left to relax for a period of $t_{rel}=120\text{s}$ and relaxation was calculated as the relative drop in reaction force over the given time period. The sample was then unloaded and left to relax for a second relaxation period of $t_{rel}=120\text{s}$. The height of the relaxed sample was measured with a ruler to determine the elastic recoil of the sample. Using the same procedure, the sample was compressed for a second time up to a peak force of $F_2=1000\text{N}$ ($\sigma_{comp}=3.18\text{MPa}$) in order to investigate compression properties of a pre-compressed sample, mimicking the clinical conditions of repeated compression through impaction. A photograph of the experimental set-up can be seen in figure 4.2. Graft compression stresses used were comparable to the range of stresses applied in other studies on compressive properties of morsellised bone graft (0.55MPa to 2.75MPa)^[225, 226].

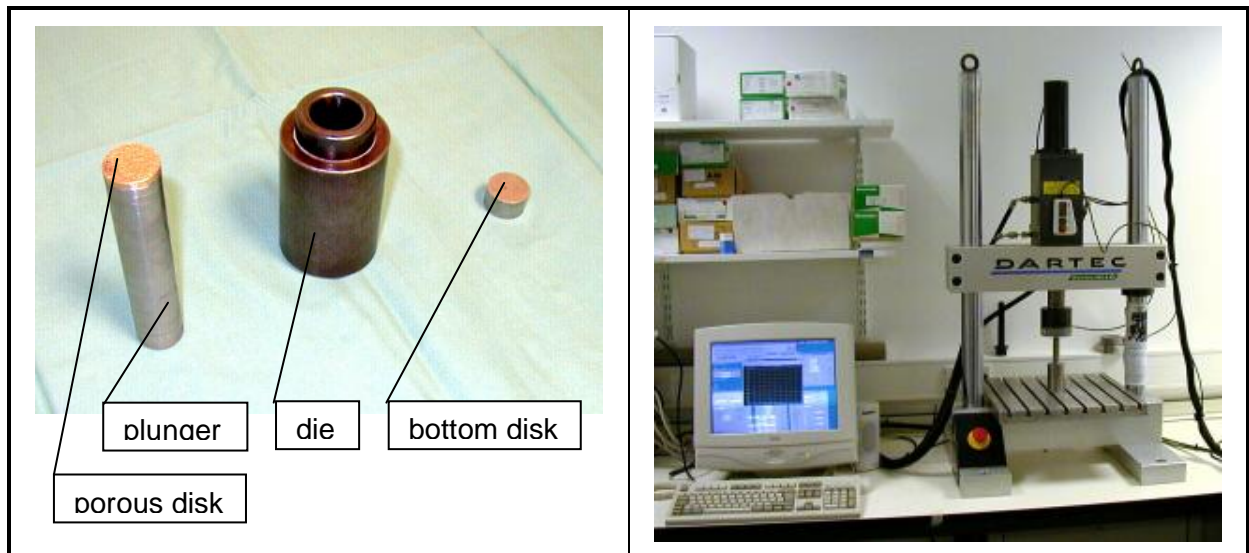


Figure 4.2: Die, plunger capped with porous disk and bottom disk. Die-plunger mounted in a Dartec HC10 test machine with computer-based control and data acquisition.

The experimental protocol, schematically shown in figure 4.1, can be summarised as follows:

1. Measuring graft volumes $V= 10\text{cm}^3$
2. Charging die with sample
3. Static pre-compression with mass $m= 1\text{kg}$
4. Measurement of start height h_{start}
5. Quasi-static compression at $v_{comp}= 2\text{mm/min}$ (ceramic) or 3mm/min (bone, mixes)
6. Compression stop at $F_1= 500\text{N}$
7. Relaxation for $t_{rel}= 120\text{s}$
8. Unloading sample to $F_0= 0\text{N}$ and second relaxation for $t_{rel}= 120\text{s}$
9. Measurement of new start height h_{start}
10. Second compression up to $F_2= 1000\text{N}$ (identical steps 3-7)

4.2 Materials

The die-plunger test offers simplicity, reproducibility, low graft volume consumption and derives comparable fundamental compression properties. This make it a suitable experiment to establish a mechanical database for variously prepared human bone grafts, different xenografts for *in-vitro* experiments, the entire range of HA/TCP ceramic graft substitutes and bone/ceramic graft mixes. Morsellised human bone graft as the gold standard material for clinical impaction grafting was tested and its properties were varied by using different bone mill types and blades, various preparation and storage methods. Human graft was tested fresh

from the mill, sterilised with γ -irradiation or formalin fixed, washed and dried or after multiple freeze-thaw cycles.

Ovine bone graft was used as the main *in-vitro* experimental bone graft in this study so that it was compression tested varying some of the same parameters as with the human bone in order to establish a correlation between the mechanical behaviour of both. In addition, bovine bone graft was tested but only fresh graft from defrosted bovine humerae morsellised with a Howex bone mill (coarse and fine blade) was used for reasons previously described in section 3.2.

The hydroxyapatite/tri-calciumphosphate graft substitutes were tested as pure materials and in various mixes with fixed ovine graft. The entire bandwidth of ceramic parameters altered as described in section 3.3 was investigated (chemical composition, sintering temperature, porosity levels and size).

Human bone	Ovine bone	Bovine bone	Ceramic	Graft mix
Fresh from frozen	Fresh from frozen		Porosity 0% 25% 50%	Mixing ratios: 2:1 b/c 1:1 b/c 1:2 b/c
γ -irradiated 2.5MRad				
γ -irradiated 5.0MRad			Size: Small 1-2mm Medium 2-4mm Large 4-6.3mm	
Formalin fixed	Formalin fixed			
Dried			T_{sint} : 1050°C 1150°C 1200	
Washed & dried	Washed & dried			
5 freeze/thaw cycles				
Howex mill fine blade		Howex mill fine blade	Composition: 80:20HA/TCP, 50:50 HA/TCP 20:80 HA/TCP	
Howex mill coarse blade		Howex mill coarse blade		

Table 4.1: Graft materials compression tested using the die-plunger experimental protocol. All bone grafts were morsellised with the Norwich[®] unless stated otherwise.

Bone and ceramic grafts were mixed at volumetric ratios of 2:1 bone/ceramic (b/c), 1:1 b/c and 1:2 b/c. All bone, ceramic and mixed grafts were prepared and mixed in large volumes prior to testing in order to reduce the variability of sample preparation. Six samples per parameter set were tested and unpaired student-t tests were performed on the data for statistical analysis (see appendix). Table 4.1 list the materials configurations tested in compression.

4.3 Data evaluation

Compressive properties were analysed by deriving a secant compression modulus and a percentage relaxation from the force-time curve as shown in figure 4.3. The slope of a straight line between the strains recorded at 25N, discarding settling effects, and at the peak load of 500N was defined as the compression secant modulus. Relaxation was calculated as the relative percentage drop of the reaction force two minutes after loading was stopped at the peak load of 500N. A two minute period was sufficiently long for a characteristic property differentiation as the reaction force declined at an exponentially constant rate. Recoil was calculated as the relative increase in sample height after the sample was completely unloaded for a time period of two minutes.

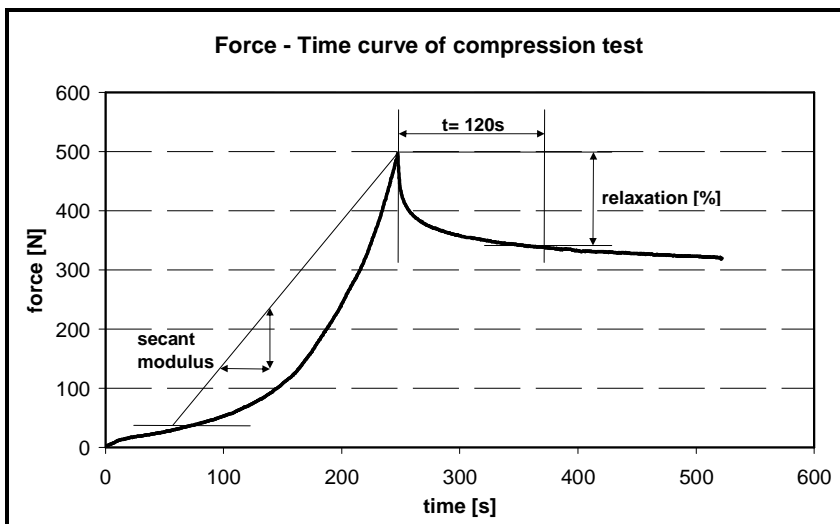


Figure 4.3:

Derivation of compression secant modulus and relaxation value.

Relaxation and recoil were calculated to quantify in some way the plastic and viscoelastic deformation properties of graft materials which are of great clinical relevance. First, the dampening effect of a viscoelastic deformation behaviour influences the ratio between impaction force and energy delivered and thus the stability providing compaction level achieved. It also influences the impaction feedback to the surgeon and thus his subjective assessment of the impaction level reached. Secondly, graft recoil and relaxation can over a short time period change the dimensions of the medullary canal created and the stiffness or load bearing capacity achieved immediately after impaction. In the case of an altered canal geometry due to recoil the critical parameter, cement mantle thickness, is influenced. In impaction grafting cement mantle thickness is defined by the implant chosen pre-operatively and the phantom prosthesis used for the final impaction blows. The phantom prosthesis is oversized to create the cement mantle gap between the medullary canal and the implant and

when it is removed after impaction into the biomechanically required position even small levels of recoil can affect the cement mantle thickness as the optimum measures only ca. 2mm in width. In theory high levels of recoil could even affect the implant position as an expanding graft mantle changes the position originally created by the phantom. In the long term recoiling graft might even push the implant in the proximal direction. In the case of relaxation, graft stiffness and stability are affected and the correlation between original impaction intensity and stability changes over time. High or variable relaxation of an impaction grafting material can thus lead to instability and to surgical misjudgement about stability on the basis of achieved impaction levels.

Data analysis of the second compression phase to a peak force of 1000N was done in a similar way but two secant compression moduli were calculated. The first value was again calculated between the strains recorded at 25N, excluding settling effects, and at the 500N peak load of the first compression. This modulus was documented to compare original stiffness and the increase in stiffness resulting from the first compaction, a clinically important graft property during multiple blow impaction. The second compression modulus was calculated as the gradient of the secant between 600N and the 1000N peak force. It was recorded to discover how differences in graft stiffness measured at lower stresses compare to graft stiffness at higher stresses and whether they correlate.

Six samples per group were tested and for statistical analysis unpaired two-tailed student t-tests were performed on the data. The mechanical properties quantified are in summary:

- Secant stiffness modulus 1st compression 0-500N E_1 [MPa]
- Compression stiffness secant modulus 2nd compression 0-500N E_2 [MPa]
- Compression stiffness secant modulus 2nd compression 600N-1000N E_3 [MPa]
- 120s relative relaxation after 1st compression 0-500N Rel_1 [%]
- 120s relative recoil after 1st compression 0-500N R [%]
- 120s relative relaxation after 2nd compression 0-1000N Rel_2 [%]

4.4 Results

4.4.1 Results - bone grafts

- **Human graft**

Figure 4.4 shows the typical force versus time curves for a human bone graft during initial compression from 0-500N (black line) and secondary compression from 0-1000N (grey line). The bone was freshly morsellised with a Norwich mill and chosen as a representative example illustrating the qualitative compression behaviour of morsellised bone grafts.

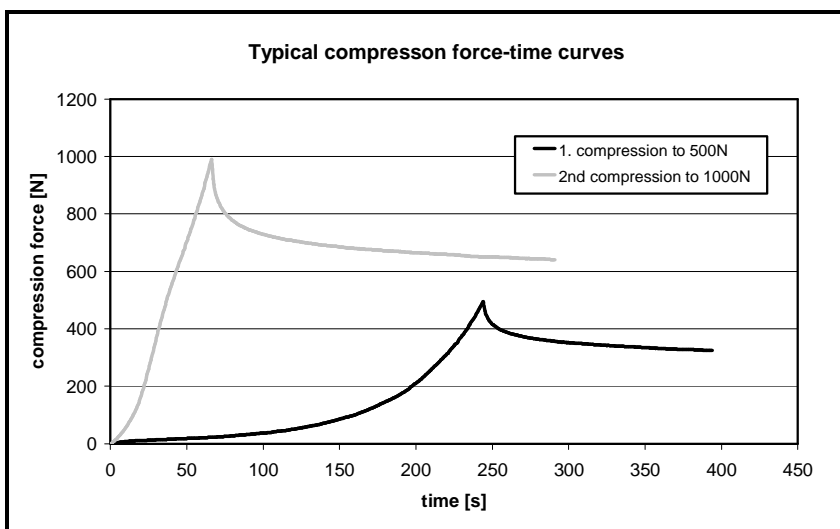


Figure 4.4:

Typical compression force versus time curves for human bone graft freshly milled with a Norwich bone mill. Black line: 1st compression 0-500N; grey line: 2nd compression 0-1000N.

Qualitatively all bone graft samples showed identical compression behaviour. During the first compression to a 500N maximum load, the force increased exponentially to the peak. Once the crosshead of the test machine was stopped and held in position the force dropped exponentially by approximately 30% to 40% during a two minute period. When such a pre-compressed sample was then loaded for a second time to a peak force of 1000N, the bone graft responded in a stiffer manner than during initial compression. When the peak force of the initial compression was exceeded at 500N more or less pronounced graft dependent decrease in the gradient of the stress-strain correlation was noticed. However, this gradient was still much higher than during the initial 0-500N compression. Once the original peak load was exceeded, the stress-strain relation became linear. As can be seen in figure 4.5 for a typical bone graft sample, between 600 and 1000N the linearity of the force-strain curve produced the linear regression coefficients R^2 greater than 0.99 for all bone samples. During the second relaxation phase, after the crosshead had stopped at a 1000N peak load, the reaction force again dropped by ca. 30%-40% within a two minute period. Three stiffness

values were calculated to quantitatively distinguish the graft materials of identical qualitative properties. These were the secant moduli for the initial 0-500N compression, the secondary 0-500N compression and for the continued 500-1000N compression. Relaxation from both the 500N and the 1000N peak and the recoil after the 500N compression were also compared.

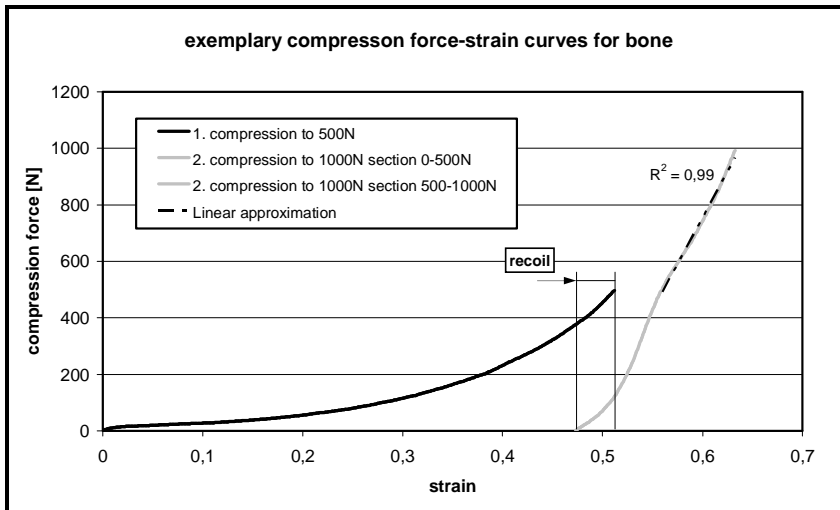


Figure 4.5:

Superimposed force vs. strain curves of a typical bone graft sample during initial 0-500N (black) and secondary 0-1000N compression (grey).

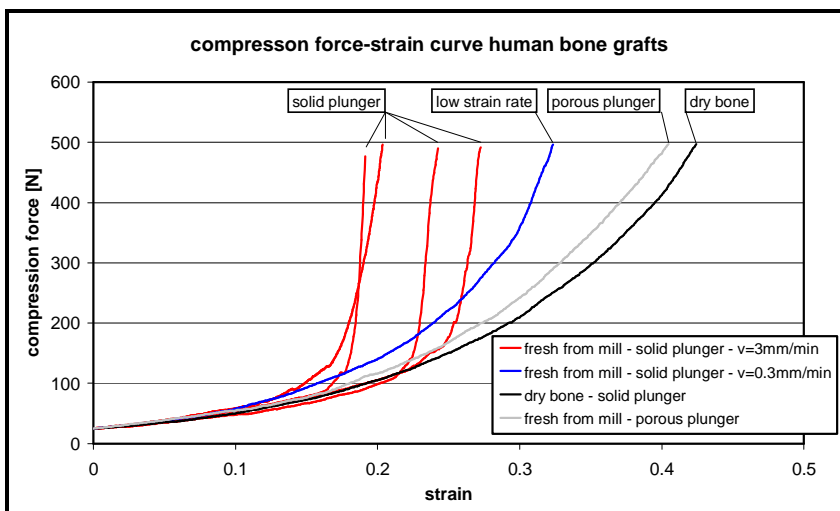


Figure 4.6:

Force-strain curves of human bone graft compressed with a solid plunger (fresh, dry, standard and low strain rate) and with a porous plunger (fresh).

Figure 4.6 shows how the force-strain response of bone grafts is affected by the use of a solid or a porous plunger. Compression of fresh and thus bloody morsellised bone graft with a solid plunger resulted in a sudden and steep ramp-like increase in stiffness once ca. 100N of force was exceeded. The maximum strains recorded at the peak load varied greatly. Reducing the strain rate to 10% of the standard at $v_{comp} = 0.3\text{mm/min}$, the ramping effect was much less pronounced but the maximum strain recorded at the peak load and thus the secant stiffness modulus calculated was still much higher than values recorded for dried bone tested with a solid plunger and fresh bone tested with a porous plunger. During the slow strain-rate compression blood was squeezed out at the bottom of the die and at the top between plunger

and die. A porous plunger was consequently used for all bone grafts and bone/ceramic mixes where any level of blood or water from graft fixing or washing could have been present.

In surgery, the preparation, storage and sterilisation methods of bone grafts vary greatly. The great influence of the bone mill type on the compression properties of freshly morsellised human bone graft is represented in figure 4.7. Secant moduli of human bone morsellised with the Norwich mill ranged from 3.50MPa to 3.75MPa with an average value of 3.65MPa and a standard deviation of less than 3% (table 4.2). As can be seen from the force-strain curves, human bone prepared with the coarse blade of the Howex mill was highly significantly stiffer ($p=6.9\times 10^{-7}$) with moduli calculated between 4.04MPa and 4.25MPa and an average value of 4.14MPa (table 4.2). The stress-strain curves also show the lower stiffness variability of the Howex against Norwich milled graft with standard deviations of only 1.9% of the average. The same situation was observed during the secondary compression to a 1000N peak load (figure 4.8). Morsellising human bone with the Howex mill led to a more stable and less variable graft than using the Norwich mill. The average stiffness calculated for the secondary 0-500N re-compression phase increased to 10.66MPa for Norwich milled bone and to 12.54MPa for the Howex milled graft resulting again in significantly different grafts ($p=0.0153$). When the compression force exceeded the initial peak of 500N and entered the stress-strain correlation entered the linear phase, the average compression modulus for Norwich milled bone was 12.02MPa and for the Howex milled graft was 13.98MPa (table 4.2), a highly significant difference ($p=0.0016$). Standard deviation was again lower for the Howex milled graft with 9.0% for the 0-500N compression and 6.7% for the 500-1000N compression versus 12.9% and 7.0% for the Norwich milled bone respectively. However, changing the blade of the Howex mill from coarse to fine produced no statistically significant difference in stiffness with the moduli averaging 4.14MPa for the coarse and 4.04MPa for the fine blade (table 4.2).

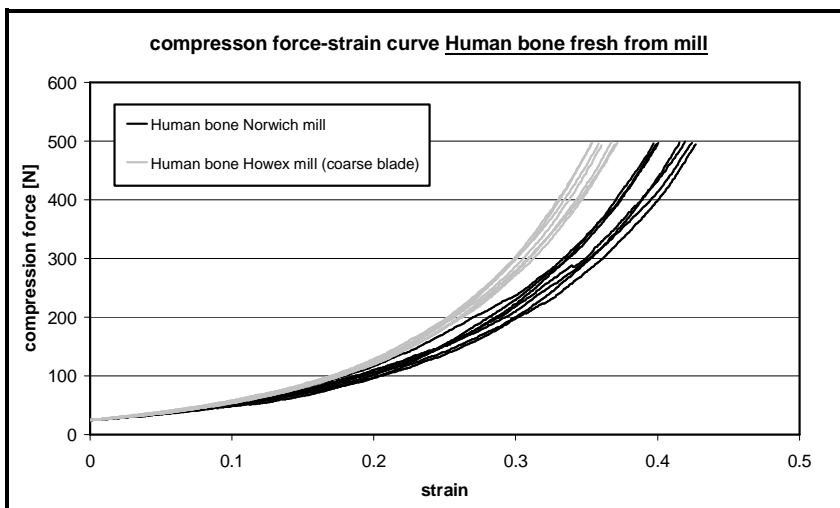
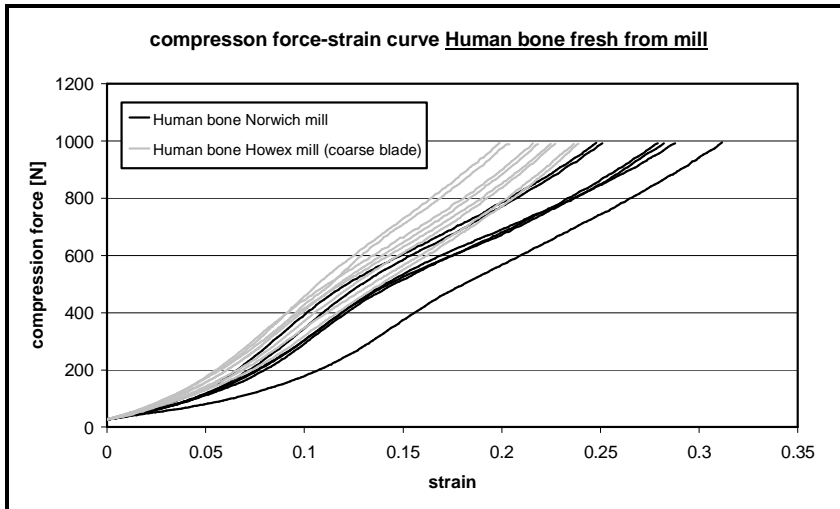


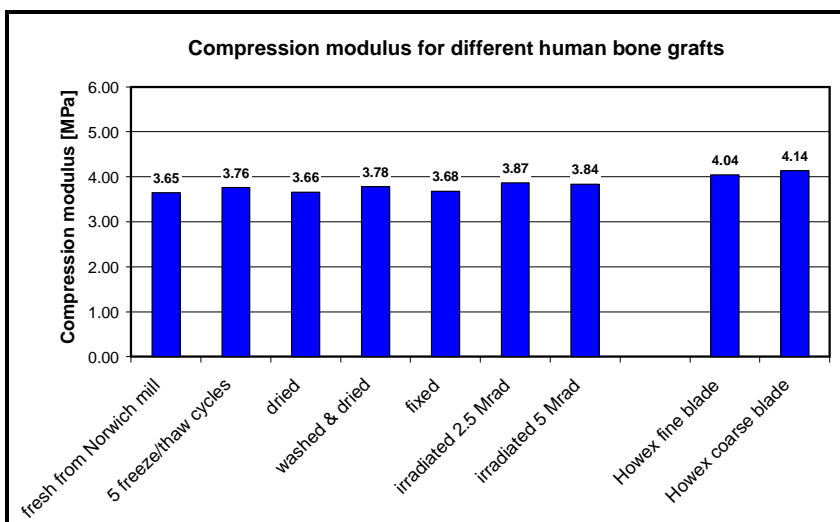
Figure 4.7:

Force-strain curves of human bone grafts freshly milled with either the Norwich or the Howex (coarse blade) bone mill. Initial compression to 500N peak load.

**Figure 4.8:**

Force-strain curves of human bone grafts freshly milled with either the Norwich or the Howex (coarse blade) bone mill. 2nd compression to 1000N peak load.

The influence of other common bone preparation, storage or sterilisation methods on graft stiffness and relaxation during initial compression is documented in figure 4.9 and 4.10 respectively. The moduli for grafts prepared with the Norwich mill ranged between 3.65MPa for fresh bone and 3.87MPa for bone sterilised with a 5MRad irradiation dose. However, the statistical significance of the different averages is below 99% for all comparisons of Norwich milled grafts and even below 95% when non-irradiated human grafts are compared only. This suggests that the compression behaviour of human bone graft is, apart from irradiation, unaffected by treatment, storage and sterilisation methods tested. As described above, only using the Howex mill produced noticeably stiffer grafts (fine blade: 4.04MPa, coarse blade: 4.14MPa), a difference of statistical significance to Norwich milled grafts for all but the 2.5MRad irradiated samples (statistical analysis in appendix). Stiffness of Howex milled graft also had the lowest variance of all bone grafts. The absolute and relative standard deviations measured 0.08MPa (1.9%) for the coarse blade and 0.07MPa (1.7%) for the fine blade compared to a range of 0.11MPa (3.0%) to 0.22MPa (6.6%) for the Norwich milled bone (table 4.2).

**Figure 4.9:**

Compression stiffness for differently prepared human bone grafts. Secant moduli calculated during initial 0-500N compression.

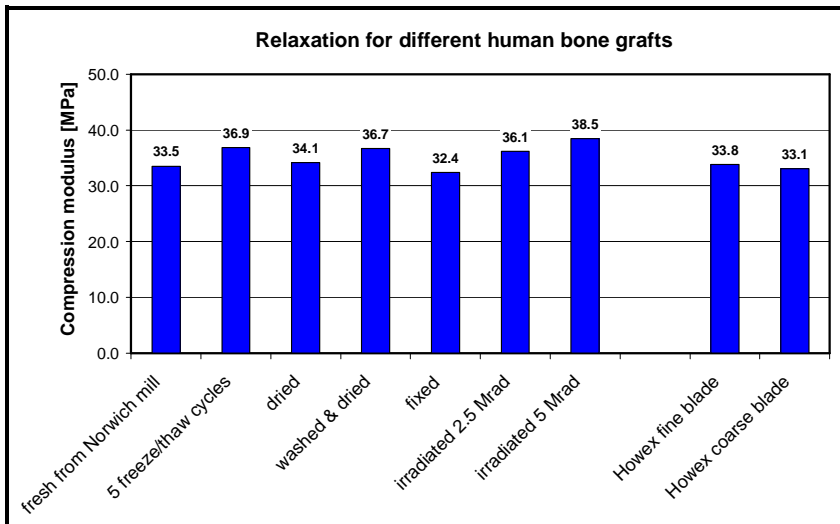


Figure 4.10: Relaxation for differently prepared human bone grafts calculated as the relative drop in reaction force from 500N peak load after a 2min period.

Comparing the relaxation behaviour of the differently prepared human bone grafts does not deliver as distinctive trends as the comparison of stiffness data. Average relaxation values ranged between 32.4% for the fixed human bone and 38.5% for the bone sterilised with a 5MRad γ -irradiation dose. Although various comparisons revealed statistically significant differences, only the extreme values of fixed and 5MRad irradiated bone consistently differed significantly ($p < 0.05$) from the majority of other grafts (statistical analysis in appendix, table 13.3). However it should be highlighted said that, for instance, the relaxation percentage for fixed human bone was not significantly different from the gold standard fresh human bone. At the same time, the Howex milled grafts that exhibited significantly higher compression moduli did not relax significantly differently relative to fresh human graft morsellised with the Norwich mill.

- **Xenografts**

Figure 4.11 compares the stress-strain curves of human bone graft with both tested xenografts, the ovine bone prepared with the Norwich mill and bovine bone morsellised with the coarse blade of the Howex mill. All four grafts were tested fresh from the mill to have a common base for comparison. While the stress-strain curves of ovine and human grafts both morsellised with Norwich mill were clearly separated, the stress-strain responses of ovine graft and human graft morsellised with the Howex mill were superimposed in a common bandwidth. The stress-strain curves of all bovine graft samples were separated from the other grafts without overlap and towards higher stiffness. These findings express themselves in the numerical stiffness analysis as summarised in figure 4.14 and table 4.2. The average compression modulus of fresh ovine graft measured 4.22MPa and was slightly higher than the

4.14MPa calculated for the Howex milled human bone but the difference was not statistically significant ($p=0.115$). However bovine bone which could only be morsellised with the Howex mill for reasons explained earlier in section 3.2 was highly significantly ($p<0.001$) stiffer than all human and ovine bone grafts. When the coarse blade was used for milling, bovine graft reached an average compression modulus of 4.91MPa. When using the fine blade, the graft is less stiff resulting in an average compression modulus of 4.51MPa ($p=0.001$) but this is still significantly stiffer than all other human and ovine graft samples.

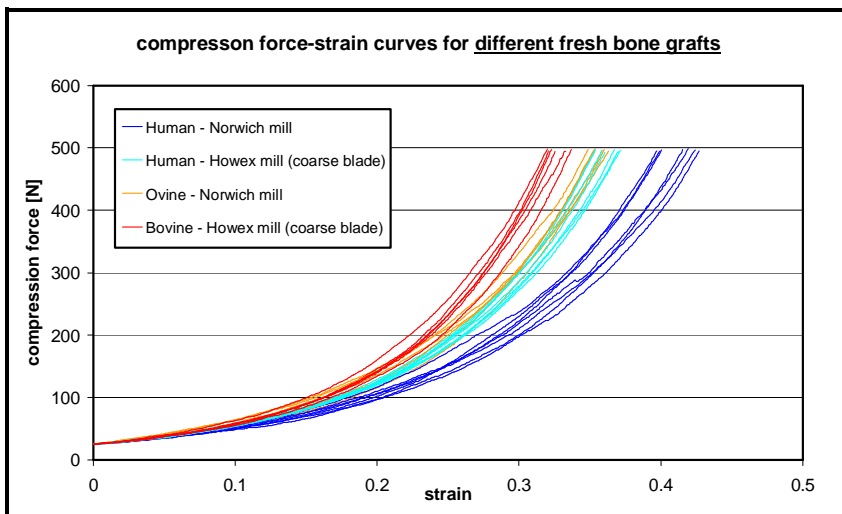


Figure 4.11: Compression force vs. strain curves for human bone graft plus ovine and bovine xenografts during the initial 0-500N compression.

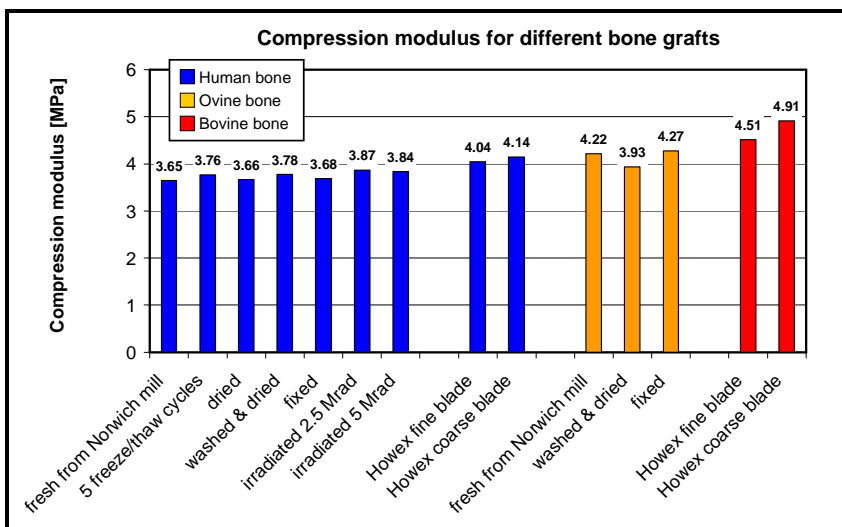


Figure 4.12: Compression moduli 0-500N for human, ovine and bovine bone prepared and stored under different conditions. Absolute and relative standard deviation given as s in [MPa] or [%] respectively.

Figure 4.12 also compares the compression moduli of the other xenografts tested with the differently prepared human grafts. Ovine bone as an experimental xenograft produced higher moduli than all Norwich milled human graft but was statistically not significantly different from the Howex milled human grafts. Bovine xenograft was up to 19% stiffer than human bone when grafts morsellised with the same Howex mill were compared and even up to 35% stiffer when fresh graft from the Norwich mill is taken as the reference. The stiffness of

human graft was not significantly affected by freezing, drying, washing or formalin sterilisation and with regards to fixation, the same was noticed for the compression moduli of ovine bone. However, contrary to the human graft's behaviour, washing and drying the ovine graft did result in a significantly decreased compression modulus (3.93MPa). With both the human and the bovine bone, using the Howex mill's coarse blade instead of the fine resulted in a higher compression modulus but the increase was significant only for the bovine graft.

	Modulus			Relaxation			Recoil
	0-500N [MPa]	SD [MPa]	SD [%]	2 min [%]	SD [%]	SD [%]	
HUMAN GRAFT							
Norwich mill fresh	3.65	0.11	3.0	33.5	1.22	3.7	10.6
5 freeze/thaw cycles	3.76	0.13	5.4	36.9	3.54	9.6	-
Dried	3.66	0.14	3.8	34.1	0.47	1.4	-
Washed & dried	3.78	0.21	5.4	36.7	1.58	4.3	12.5
Formalin fixed	3.68	0.14	3.8	32.4	0.66	2.0	13.1
Irradiated 2.5MRad	3.87	0.22	5.6	36.1	1.15	3.2	-
Irradiated 5MRad	3.84	0.15	3.9	38.5	0.44	1.1	-
Howex mill fine blade	4.04	0.07	1.7	33.8	0.93	2.8	-
Howex mill coarse	4.14	0.08	1.8	33.1	0.54	1.6	11.4
XENOGRAFT							
Ovine fresh from mill	4.22	0.07	1.7	39.6	1.83	4.6	7.7
Ovine washed & dried	3.93	0.11	2.9	31.9	1.37	4.3	-
Ovine formalin fixed	4.27	0.19	4.5	30.1	0.56	1.9	-
Bovine Howex fine	4.51	0.11	3.0	33.4	2.95	8.8	8.2
Bovine Howex coarse	4.91	0.11	3.0	32.3	1.10	3.4	7.7

Table 4.2:

Secant compression moduli, relaxation and recoil values for different bone grafts.

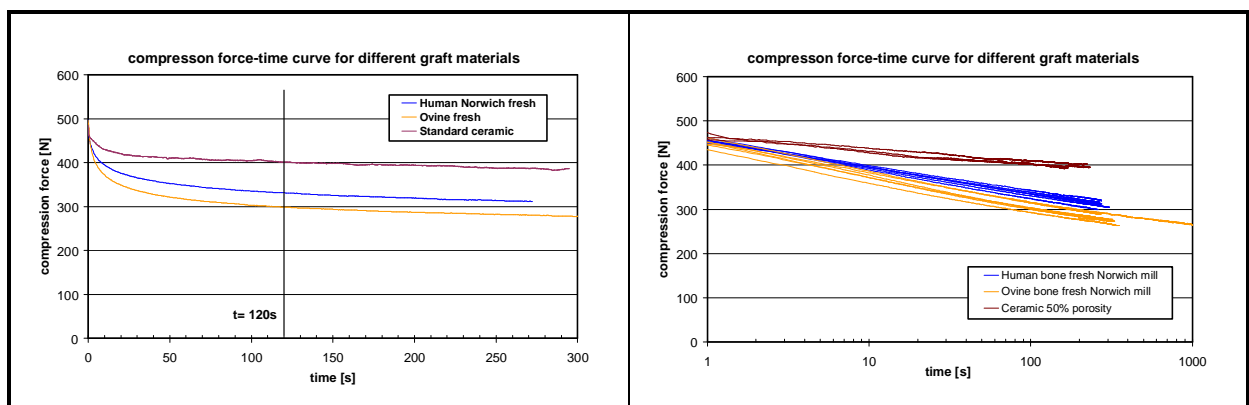


Figure 4.13: Representative time-relaxation curves for bone grafts and a typical ceramic graft substitute indicating. Left: linear time scale, Right: logarithmic time scale.

Representative for all graft materials investigated, the qualitative relaxation behaviour of a range of exemplary graft materials is given in figure 4.13. From the maximum load of 500N the reaction force of compressed human bone, ovine bone and a standard ceramic graft declined exponentially in a qualitatively identical way. Only the intensity of this decline as

quantified by the percentage drop in reaction force after a fixed time period of 120s allowed graft materials to be differentiated. When a logarithmic time scale is used these differences are reflected in different slopes of the linear force-time curves. Although the bone grafts represented in figure 4.13 represent highest and one of the lowest and average relaxation of all bone grafts response, the variability of relaxation measurements within each graft group was higher than the difference in relaxation averages. Relatively small differences in average relaxation values of high variability lead to overlapping, indistinguishable time-relaxation curves even when the grafts with the extreme relaxation averages (fixed ovine bone: 30.1%, fresh ovine bone: 39.6%) are included as seen in figure 4.14. In particular it can be seen that most xenografts such as fresh ovine or bovine bone delivered relaxation rates impossible to differentiate from human grafts commonly applied in clinic such as fresh or γ -irradiated graft.

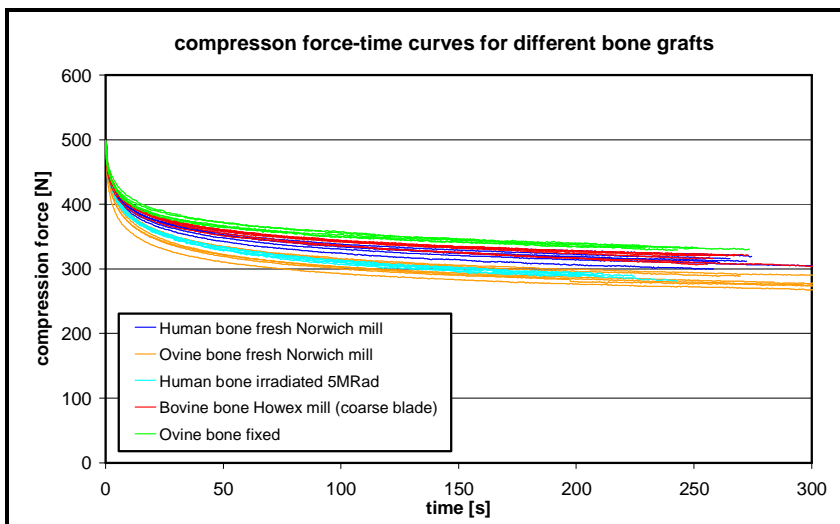


Figure 4.14:

Sets of time-relaxation curves for different bone grafts indicating the variability of results within one sample group and the bandwidth of relaxation values between different groups of graft.

Average relaxation values for the all human and xenografts are summarised in figure 4.15 which confirms that the differences in relaxation behaviour between human bone and xenografts are not as pronounced as with regards to the stiffness. Fresh human bone, regardless of bone mill type and blade size, and fresh bovine bone produced almost identical relaxation values with averages ranging between 32.4% and 33.8% only, a difference without statistical significance. In contrast, fresh ovine bone relaxed by 39.6% on average and thus behaved differently from fresh human bone. However when ovine bone was washed & dried (31.9% average relaxation) or formalin fixed (30.1% average relaxation) the relaxation was again similar to values measured for all fresh human bone variants. At the same time, certain treatment or storage methods caused the relaxation of human graft to increase in comparison to its fresh variant. The popular technique of washing & drying caused relaxation to rise to 36.7%. When γ -irradiation as the most common sterilisation method in bone banks was used

relaxation increased to 38.5%. The relaxation values recorded for differently treated human bone lay within the relaxation range measured for differently treated ovine grafts. For various combinations such as irradiated human graft or human bone after 5 freeze/thaw cycles versus fresh ovine graft, the small difference in average relaxation was not statistically significant. Whereas washing and drying or fixing human bone graft increased relaxation slightly, ovine bone reacted with a noticeable decrease in relaxation when the same treatments were applied.

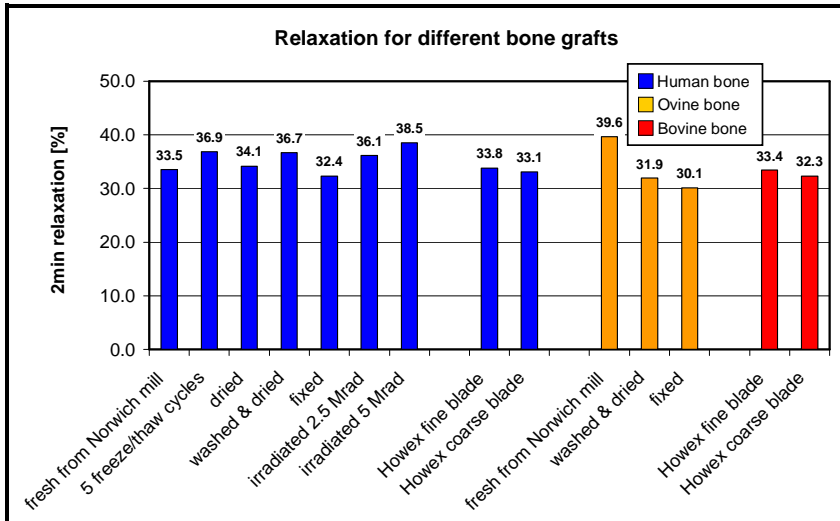


Figure 4.15:

Relaxation after the initial 0-500N compression for human, ovine and bovine bone prepared and stored under different conditions.

Recoil, as represented in figure 4.16, is the continuation of graft relaxation behaviour and elastic rebound after the sample was unloaded. After two minutes of relaxation measured with the plunger held in position of maximum strain, the samples were unloaded and the relative increase in volume or sample height over a second two minute period was measured as recoil. Standard deviation of the recoil data was high ranging from 14% to 42% of the mean values. Certain characteristics observed from the relaxation and stiffness data were also reflected in the recoil measurements. Recoil values for the human bone samples were close together ranging from 10.6% for graft freshly morsellised with the Norwich mill to 13.1% for Howex milled graft using the fine blade. For washed and dried graft, recoil was increased as was relaxation but none of the recoil differences derived within the human bone graft group were statistically significant ($p_{min}=0.147$).

Both xenografts showed less recoil than the human grafts with nearly identical averages ranging from 7.7% (fresh ovine graft and bovine graft morsellised with the coarse blade) to 8.2% (bovine graft morsellised with the fine blade). This does not correlate to their relaxation behaviour. Considering the high standard deviation of the data, only the differences between the xenografts and both Howex milled human grafts were statistically significant ($0.028 > p >$

0.0005). The recoil of both xenografts showed a reciprocal correlation with the stiffness values which were higher than human graft for both ovine and bovine bone (figure 4.12).

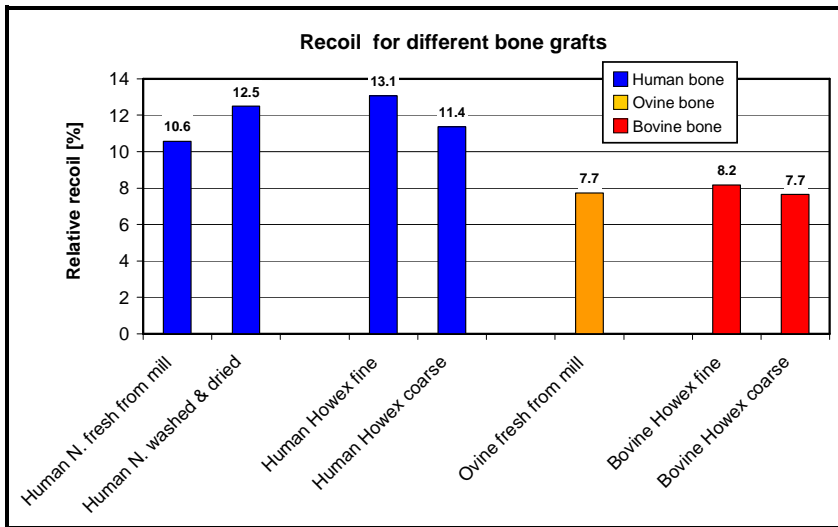


Figure 4.16:

Recoil as relative increase in volume over a two minute period after sample unloading for human bone graft plus ovine and bovine xenografts.

The compression behaviour of already compressed grafts, as relevant during multiple hammer blow impaction, was investigated by recording the stress-strain curves during a secondary re-compression from 0-1000N and is illustrated in figure 4.17. Qualitatively identical but with different slopes, the stress-strain curves of freshly morsellised human, ovine and bovine graft reflect the compression properties already identified during the initial 0-500N compression. However, certain differences are either less or more pronounced. For example during initial compression, fresh Norwich milled human graft produced the lowest stress-strain slope and thus the lowest stiffness. Again the Howex milled human graft was clearly stiffer with no overlap of stress strain curves at the 1000N peak load. Also carried forward from the initial 0-500N compression was the relative stiffness of the ovine xenograft which, except for one sample, lay entirely within the result range of the Howex milled human graft when the peak force was reached. The clearly separated stress-strain curves of bovine graft recorded during the initial 0-500N compression were no longer observed during the second loading. Still giving the highest compression moduli overall, the stress-strain responses were much closer to both ovine xenografts and the Howex milled human grafts. Table 4.3 differentiates the described behaviour more clearly by comparing the secant compression moduli during secondary compression for the 0-500N and the 500-1000N phase.

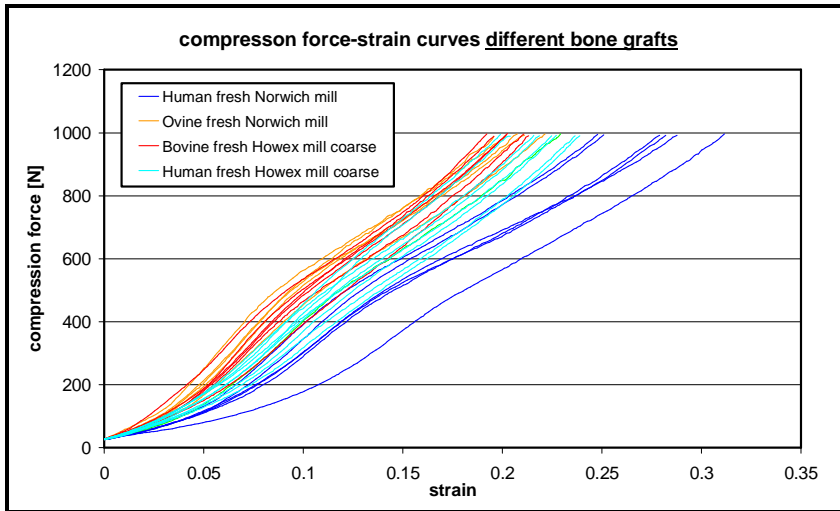


Figure 4.17: Compression force vs. strain curves for human bone graft plus ovine and bovine xenografts during secondary 0-1000N compression.

Compression moduli during the 600-1000N section were distributed in much a similar way as during the initial 0-500N compression phase and indicate a continuation of the trends measured for low forces into regions of higher loads. Fresh and washed and dried human bone graft produced lower values (12.02MPa and 11.97MPa respectively) than the Howex milled human grafts and both xenografts. The Howex milled human grafts gave moduli of 16.61MPa when bone was morsellised with the fine blade and 13.98 MPa when the coarse blade was used. As during initial compression, Howex milled human grafts were significantly stiffer than the Norwich milled alternative ($p < 0.0016$).

BONE GRAFT	Modulus									Relaxation		Recoil
	1. comp.	SD	SD	2. comp.	SD	SD	2. comp.	SD	SD	from	from	from
	0-500N	[MPa]	[MPa]	0-500N	[MPa]	[MPa]	0.5-1kN	[MPa]	[MPa]	500N	1kN	500N
	[MPa]	[MPa]	[%]	[MPa]	[MPa]	[%]	[MPa]	[MPa]	[%]	[%]	[%]	[%]
Human fresh from mill	3.65	0.11	3.0	10.66	1.38	13	12.02	0.84	7.0	33.5	32.7	10.6
Human washed & dried	3.78	0.21	5.4	10.7	0.79	7.4	11.97	0.44	3.7	36.7	36.9	12.5
Human Howex fine	4.04	0.07	1.7	10.82	0.39	3.6	15.51	0.45	2.9	33.8	34.0	13.1
Human Howex coarse	4.14	0.08	1.9	12.54	1.12	9.0	13.98	0.93	6.6	33.1	32.7	11.4
Ovine fresh from mill	4.22	0.07	1.7	15.29	1.73	11	14.63	0.81	5.5	39.6	40.7	7.7
Bovine Howex fine	4.51	0.11	2.9	14.88	1.24	8.4	18.04	0.52	2.9	33.4	33.1	8.2
Bovine Howex coarse	4.91	0.19	4.5	14.78	1.37	9.3	16.47	0.65	4.0	32.3	32	7.7

Table 4.3: Secant compression moduli, relaxation and recoil values for different bone grafts.

The average stiffness of ovine bone was calculated as 14.63MPa and thus, like during initial compression, was similar to the Howex milled human grafts; no statistical differences at the 99% confidence interval could be identified ($p_{coarse}=0.1932$, $p_{fine}=0.0421$). As found during the initial 0-500N compression, bovine bone graft was much stiffer than fresh Norwich milled bone registering compression moduli of 18.04MPa (fine blade) and 16.47MPa when the

coarse blade was used. However, the difference between the Howex milled bovine and human grafts was not as large as during the initial compression. Even so the stiffest bovine graft was still 29% stiffer than the weakest and 9% stiffer than the strongest Howex milled human graft (highly significant).

While the average standard deviation of the moduli during the initial 0-500N compression was only 2.8% and still only 4.7% during the 500-1000N phase of the secondary compression, the average standard deviation for the secondary 0-500N compression was more than 8.8% so that differences between the human grafts were only statistically significant for comparisons with grafts morsellised with the coarse blade of the Howex mill. Despite reduced differences and a lack of statistical significance in cases, even during the secondary 0-500N compression fresh Norwich milled bone had the lowest average compression modulus (10.66MPa) and both Howex milled human grafts were stiffer (fine blade: 10.82MPa, coarse blade 12.64MPa). As before, both xenografts had moduli higher than the Norwich milled bone and this time also in comparison with the Howex milled human bone and all differences were statistically significant ($p < 0.0011$). The highest modulus during secondary compression from 0 to 500N was measured for ovine bone graft but standard deviation was at 11.3% so high, that no statistically significant difference with both bovine grafts (coarse blade: 14.78MPa; fine blade 14.88MPa) could be identified.

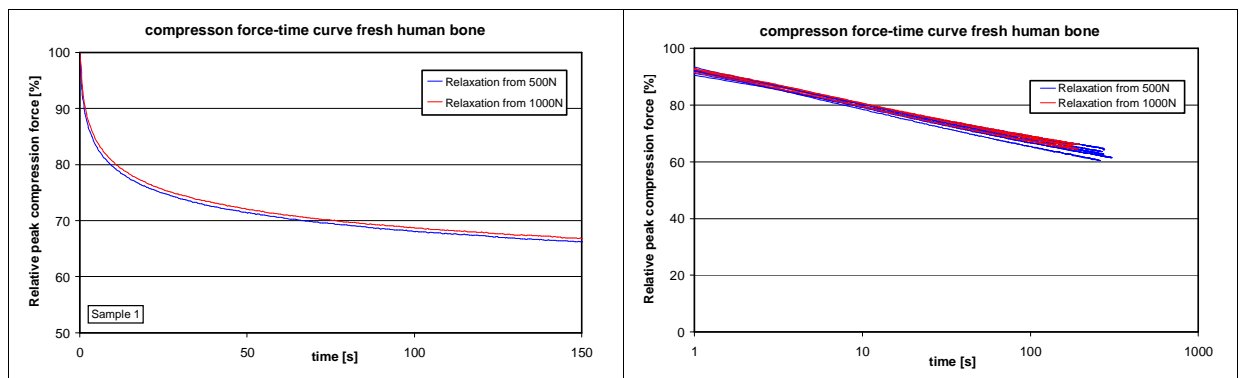


Figure 4.18: Superimposed time-relaxation curves from 500N and 1000N peak force for one typical sample (left) and all fresh human graft samples (right, logarithmic scale). The peak force was normalised to 100%.

Relaxation of the pre-compressed samples from their second peak load of 1000N was qualitatively identical to the first 500N relaxation phase. The numerical values were also almost equal on average (table 4.3) with individual samples relaxing by 0.4 percentage-points less on average after re-compression to 1000N. For illustration, figure 4.18 shows the superimposed relaxation rates from both the 500N and the 1000N peak for one representative

example of fresh Norwich milled human bone (left) and for all samples combined (right, logarithmic time scale). The standard deviation of relaxation properties between different samples is larger than the reduced relaxation between initially and re-compressed individual samples.

4.4.2 Results - ceramic graft extenders

The HA/TCP bioceramics designated as bone graft extenders behaved entirely differently from both human and xenograft bone and did not mimic their qualitative and quantitative performance under compression. Figure 4.19 represents a typical compression force versus time response for one sample of the standard ceramic configuration tested, a 80:20 HA/TCP composite with 25% porosity (medium) and 2-4mm granule size (medium) sintered at $T_{sint}=1150^{\circ}\text{C}$.

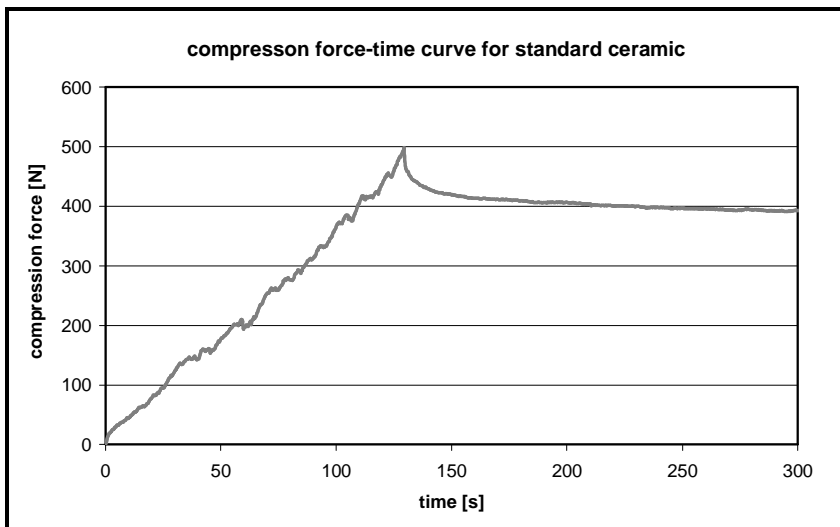


Figure 4.19:

Typical compression force vs. time curve for one sample of the standard ceramic configuration tested.

During the compression phase the stress-strain curve resembled a straight line in first approximation superimposed on a more detailed scale by sudden drops and steep rises resulting in a saw-tooth profile to the curve. When compared to figure 4.4, the qualitative and quantitative differences of this stress-strain response to the exponential stress-strain curves recorded for bone grafts become very obvious. The relaxation for ceramics was much less than for bone grafts but qualitatively, the time-dependent drop in reaction force was identical. Figure 4.20 shows relaxation curves for the bone grafts with the highest and lowest relaxation in comparison to one representative of the synthetic extender material, the standard ceramic with a high level 50% porosity. Once the plunger was stopped at 500N peak load, the

compression force decreased for bone and ceramic grafts in an exponential manner as highlighted in the right chart with its logarithmic scale. The different slopes of the curves represent the very significant difference in absolute relaxation between bone and ceramic grafts. This difference is much larger than the relatively small variations in relaxation between the human and xenograft bone.

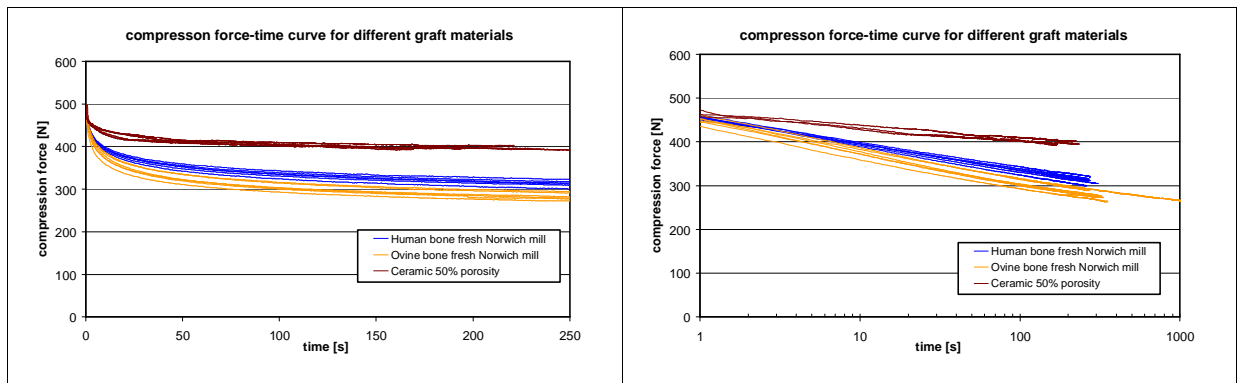


Figure 4.20: Time-relaxation curves for those bone grafts with the highest and lowest relaxation and one typical ceramic graft. Left: linear time scale, Right: logarithmic time scale.

Figure 4.21 compares the range of graft stiffness attainable with the tested variety of HA/TCP ceramics to a range of typical bone grafts. Again, the different stress-strain responses of bone (exponential) and ceramic grafts (linear with saw-tooth profile) become highlighted. With the highly porous samples the sudden drops and stress rises superimposed on the linear trend were significantly more pronounced. The maximum average compression modulus measured for all HA/TCP ceramic grafts was 29.27MPa for the non-porous material and the minimum stiffness was recorded at 7.98MPa for the highly porous material (table 4.4). This equates to an attainable stiffness range of 367% $((\text{max}-\text{min})/\text{min})$ for the HA/TCP ceramic which compares to 13% for differently prepared human grafts and 31% when the xenografts are included. As a result of the saw-tooth profile of the stress-strain curves, the standard deviation of modulus measurements was higher for the ceramics than for the bone grafts. The stiffness values calculated for the ceramic granules produced standard deviations between 10.2% (50% porosity and $T_{\text{sint}}=1050^{\circ}\text{C}$) and 16.7% (0% porosity) of the averages. In comparison, the bandwidth of standard deviations measured for the bone graft samples varied only between 1.7% (human Howex fine) and 5.6% (human irradiated 2.5MRad) of the average values.

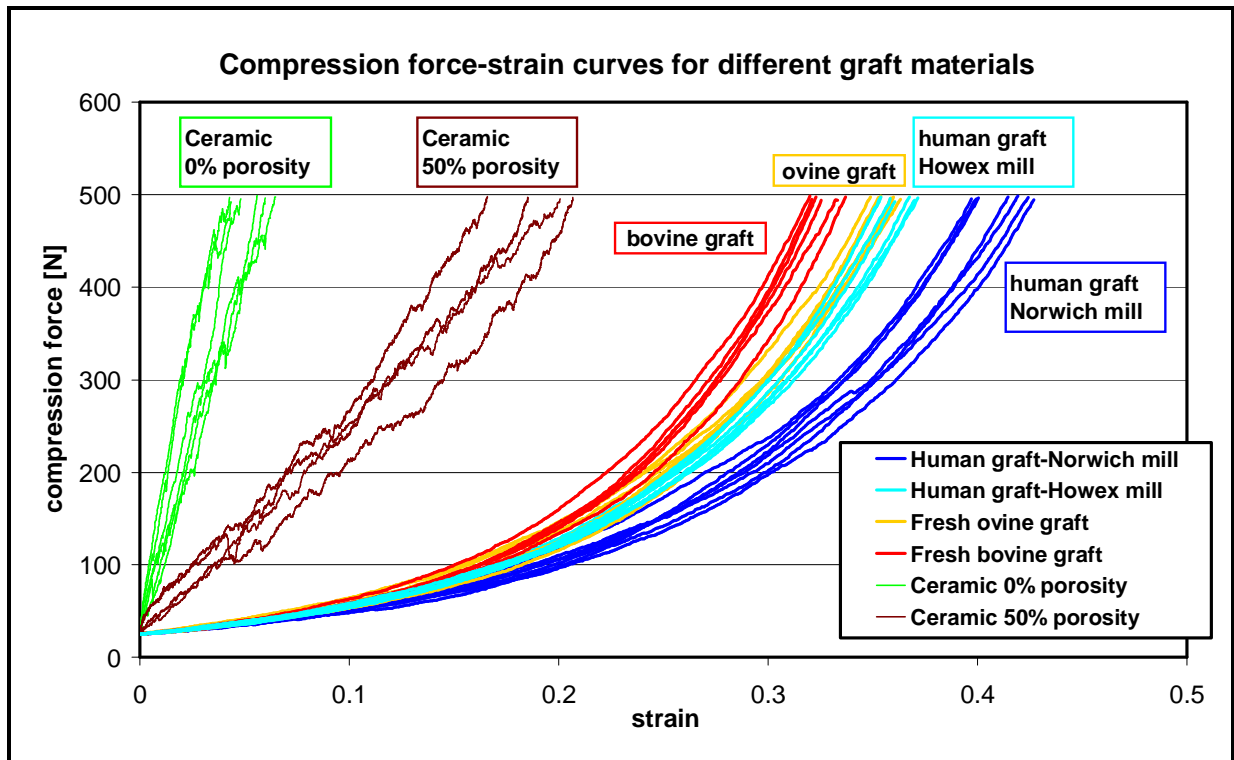


Figure 4.21: Compression force-strain curves for two HA/TCP ceramic graft configurations with extreme stiffness properties in comparison to typical bone grafts.

GRAFT MATERIAL	Modulus									Relaxation		Recoil
	1. comp. 0-500N [MPa]	SD [MPa]	SD [%]	2. comp. 0-500N [MPa]	SD [MPa]	SD [%]	2. comp. 0.5-1kN [MPa]	SD [MPa]	SD [%]	from 500N [%]	from 1kN [%]	from 500N [%]
Human Howex coarse	4.14	0.08	1.9	12.54	1.12	9.0	13.98	0.93	6.6	33.1	32.7	11.4
Ovine fresh from mill	4.22	0.07	1.7	15.29	1.73	11	14.63	0.81	5.5	39.6	40.7	7.7
Ceramics												
0% porosity	29.27	4.89	17	162.0	29.7	18	33.4	7.9	24	19.4	16.5	0.42
25% porosity	16.11	2.17	14	149.9	31.9	21	17.0	0.3	2	18.7	17.3	0.77
50% porosity	7.98	0.82	10	114.5	32.2	28	15.1	0.6	4	18.9	16.3	0.10
T _{sint} = 1050°C	10.69	1.09	10	103.0	50.7	49	19.5	1.6	8	18.7	17.1	0.26
T _{sint} = 1200°C	22.78	5.74	25	186.2	45.4	24	24.4	4.3	18	19.3	17.8	0.44
Small	23.18	2.60	11	130.3	38.2	29	24.7	3.9	16	18.9	16.3	0.40
Large	13.68	2.03	15	109.8	38.3	35	16.2	3.1	19	19.0	17.0	0.32
20:80 HA/TCP	14.42	1.45	10	103.2	19.2	19	17.0	1.6	10	19.5	16.8	-
Pure HA, 68% porosity	3.71	-	-	56.5	-	-	12.5	-	-	21.2	21.1	-

Table 4.4: Secant compression moduli, relaxation and recoil values for different ceramic grafts.

The standard HA/TCP ceramic and its variants were produced by TCM Associates, UK using the method described in section 3.3. In order to expand analysis of synthetic graft extenders beyond this limited focus, another ceramic material from an alternative manufacturer aimed at replacing bone graft in impaction grafting was tested for comparison. Manufactured by a non-disclosed method, the pure HA offered a very high (68%) and interconnected porosity. This

ceramic configuration expanded the stiffness range attainable by ceramic grafts even further. as figure 4.22 shows. The stress-strain curves of the highly porous HA were much less steep than the least stiff HA/TCP variant and even those of Howex milled human graft. Mimicking the compression behaviour of human bone graft, the highly porous HA it compressed exponentially with increasing stiffness. The average modulus was only 3.71MPa compared to 4.14MPa measured for the Howex milled human graft. Comparing the maximum modulus of the non-porous HA/TCP ceramic graft (29.27MPa) with the stiffness of the highly porous HA shows that the stiffness attainable with ceramic grafts can be manipulated within a range of 690%. With the highest porosity of all tested ceramics, the stress-strain curves of pure HA showed an even more pronounced saw-tooth profile than the 50% porous HA/TCP. Sudden drops in reaction force during compression measured up to 38N or 13%.

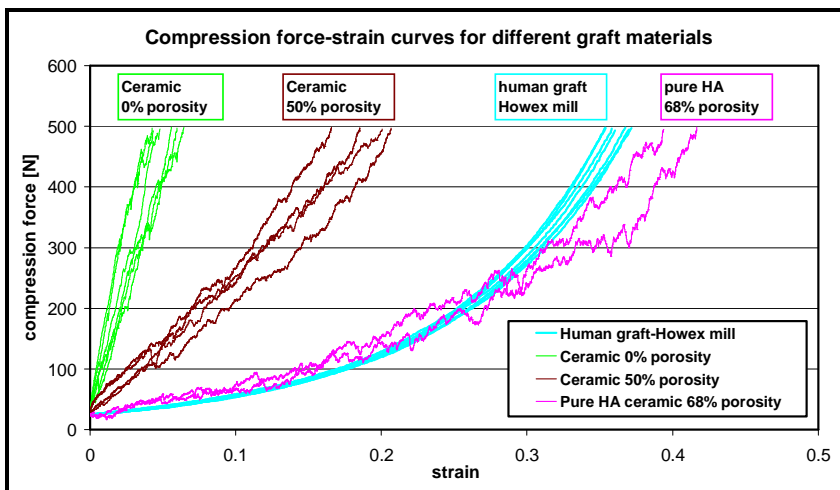


Figure 4.22:

Compression force vs. strain curves for two HA/TCP ceramic graft configurations and a highly porous HA with extreme stiffness properties in comparison to human bone graft.

Figure 4.23 and table 4.4 summarise the average compression moduli calculated for all ceramic grafts during the initial 0-500N compression. For reference the stiffness values of some distinctive human and xenografts are included. It can be seen that the major ceramic parameters which were altered - porosity, particle size and sintering temperature - had a clear and highly significant effect on the compression modulus. The stiffest sample was the non-porous HA/TCP composite ceramic. Increasing the porosity had the strongest effect of all parameters on the mechanical performance of granular ceramic grafts. The compression modulus decreased by nearly 50% from 29.27MPa to 16.11MPa when 25% porosity was introduced and it dropped further to 7.98MPa when the 50% porous graft was tested. The pure HA sample with its interconnected 68% porosity continued this trend towards a minimum compression modulus of 3.71MPa. This value was lower than most human bone grafts tested.

Like porosity, increasing the particle size from small (1-2mm) to medium (2-4mm) and large (4-6.3mm) decreased the compression modulus. However, the size-stiffness correlation was weaker than the effect of porosity. The maximum modulus was recorded for small ceramic particles at 23.18MPa and it dropped to 13.69MPa for large granules.

Increasing the sintering temperature had the opposite effect on stiffness than that of porosity and size. Increasing the sintering temperature also lead to an increase in compression modulus and this correlation was of similar strength than the reciprocal effect of particle size. Stiffness increased from 10.69MPa for the low sintering temperature ($T_{sint}=1050^{\circ}\text{C}$) to 22.78MPa for the highest temperature ($T_{sint}=1200^{\circ}\text{C}$).

Reversing the chemical composition of the ceramic graft from 80:20 HA/TCP to 20:80 HA/TCP had only a relatively small effect on the compression modulus. On average it decreased from 16.11MPa (80:20 HA/TCP) to 14.42MPa (20:80 HA/TCP), a 10% reduction which does not indicate a statistically significant difference ($p=0.11$). Despite the high standard deviations, the remaining differences between ceramic compression moduli were all significant ($p<0.05$) except when medium and large particles were compared ($p=0.063$).

The mechanically weakest HA/TCP composite ceramic was approximately twice as stiff as the human bone grafts and significantly stiffer than all xenografts. The highly porous pure HA ceramic had a lower compression modulus than all but one human graft (Norwich mill). When the exponentially rising stress-strain response of the bone grafts is considered and stiffness is analysed as a tangent modulus near the peak load, the relatively lower stiffness of a very porous ceramic graft material becomes even more pronounced (figure 4.22).

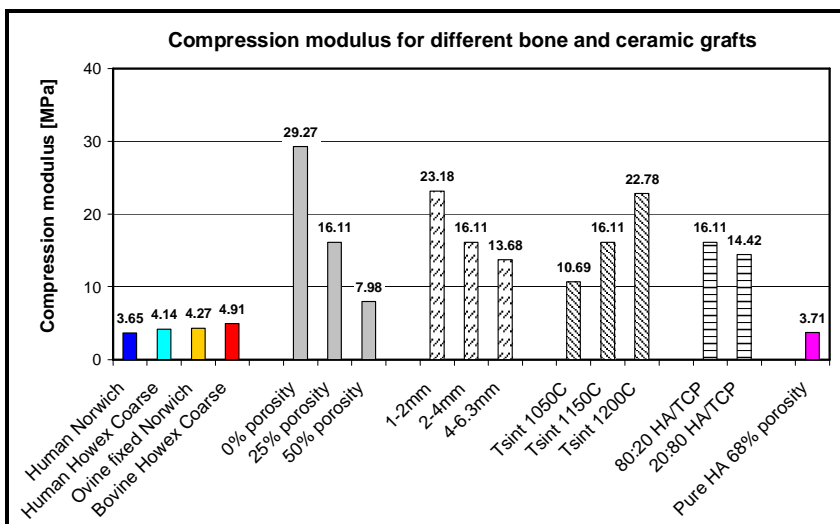


Figure 4.23:

Compression moduli for different ceramic graft materials during the initial 0-500N compression compared to typical bone grafts.

The relaxation behaviour of the granular ceramic grafts was qualitatively identical to human and xenograft bone but significantly less as previously shown in figure 4.20. Relaxation as the percentage drop in reaction force two minutes after plunger movement was stopped ranged only between 16.8% and 22.0% for all ceramic samples (figure 4.24, table 4.4). Average values were even closer to each other ranging between 18.7% and 19.5% for the HA/TCP composite ceramics and 21.2% for the highly porous pure HA. Excluding the two pure HA samples in the statistical analysis, all differences in relaxation were not statistically significant ($0.22 < p < 0.98$) in a two-sided unpaired student t-test. Thus, despite the strong influence of ceramic porosity, size and sintering temperature on stiffness, relaxation remains unaffected.

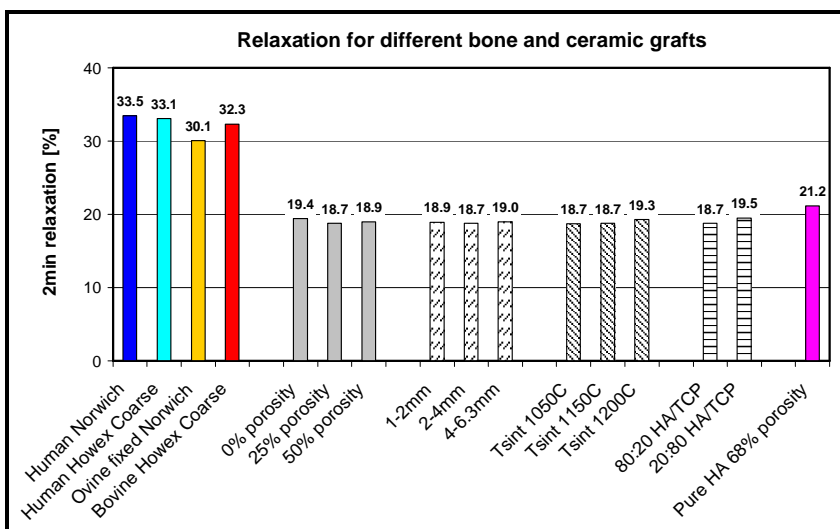


Figure 4.24: Relaxation for different ceramic graft materials during the initial 0-500N compression compared to typical bone grafts.

During secondary compression to a peak load of 1000N, the granular ceramics continued the linear stress-strain relationship with a superimposed saw-tooth profile already observed during the initial 0-500N compression. For one typical sample of the standard ceramic (80:20 HA/TCP, 25% porosity, 2-4mm particle size, $T_{sint}=1150^{\circ}\text{C}$), figure 4.25 superimposes the force-strain signals of the initial 0-500N compression and the secondary 0-1000N compression and illustrates the described continuation of the linear stress-strain response. Also visible is the elastic recoil which, when related to the sample height at maximum compression measured 0.77% on average for the standard ceramic configuration and 0.67% for the specific sample shown here.

Figure 4.26 summarises the recoil measurements of all tested ceramics in a bar chart. Recoil or the elastic recovery was here calculated as the increase in sample height relative to the sample height at maximum compression. Despite nearly equal relaxation values (figure 4.24), average recoil varied between 0.1% (50% porosity) and 1.0% (20:80 HA/TCP) for all

samples. Due to the high standard deviations which ranged between 39% and 128% of the average recoil values, most differences between the ceramic configurations compared were not statistically significant. However, when the extremes of one altered parameter are compared, a consistent trend could be identified. Stiffer ceramics (0% porosity, small 1-2mm particle size and $T_{sint}= 1200^{\circ}\text{C}$) show more elastic recoil than the less stiff ceramics (50% porosity, large 4-6.3mm particle size and $T_{sint}= 1050^{\circ}\text{C}$). In comparison, recoil for human bone grafts (figure 4.16) varied between 10.6% (fresh human Norwich) and 13.1% (fresh human Howex fine) and thus was more than ten times higher.

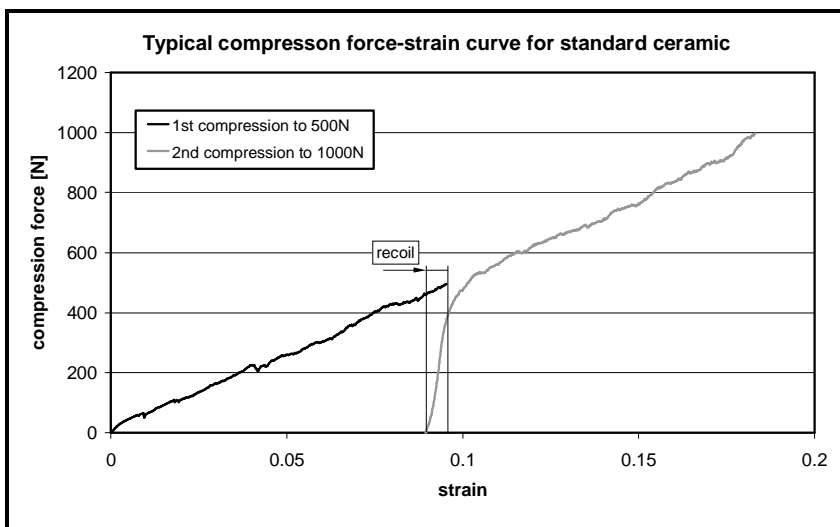


Figure 4.25:

Superposition of the force - strain curves of a typical ceramic graft for the initial 0-500N compression and the secondary 0-1000N compression.

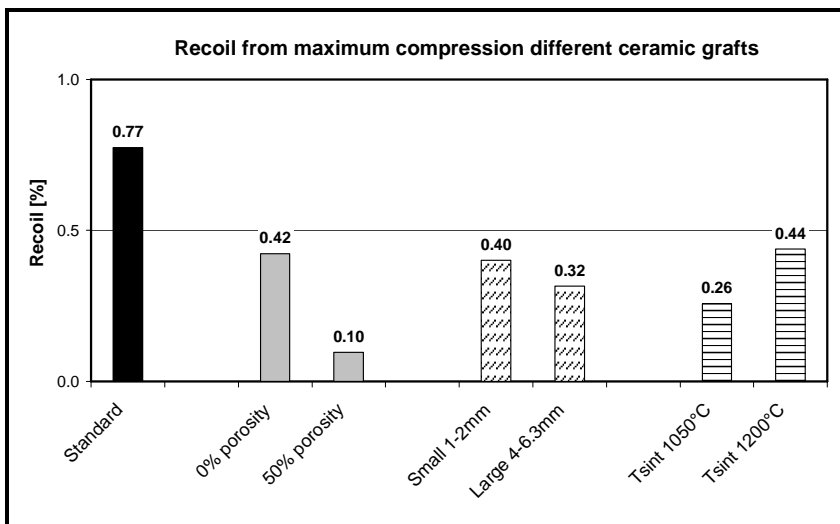


Figure 4.26:

Recoil of ceramic samples after initial compression from 0-500N calculated as the relative increase in sample height from maximum deflection after unloading.

When the recoil is calculated in relation to the maximum displacement and not to the sample height at maximum compression, the recoil values of the ceramics increase because of their small total displacement relative to bone. Figure 4.27 displays recoil relative to maximum displacement (right) in comparison to the recoil relative to minimum height and it can be seen

that above observations remain valid for the relative comparison of ceramic grafts. In addition, recoil values for bone grafts are included for reference. The absolute values for ceramic grafts increase more than for the bone grafts and differences between the ceramic configurations become more pronounced. The range of differently defined recoil measured from 0.5% (50% porosity) to 6.6% (0% porosity) or 7.5% (standard ceramic). Recoil for bone grafts remained significantly higher ranging from 9.3% (Howex coarse milled bovine bone) to 15.9% (Howex fine milled human bone). Due to the high standard deviations, statistical significance could not be proven for most comparisons within the ceramic and bone groups.

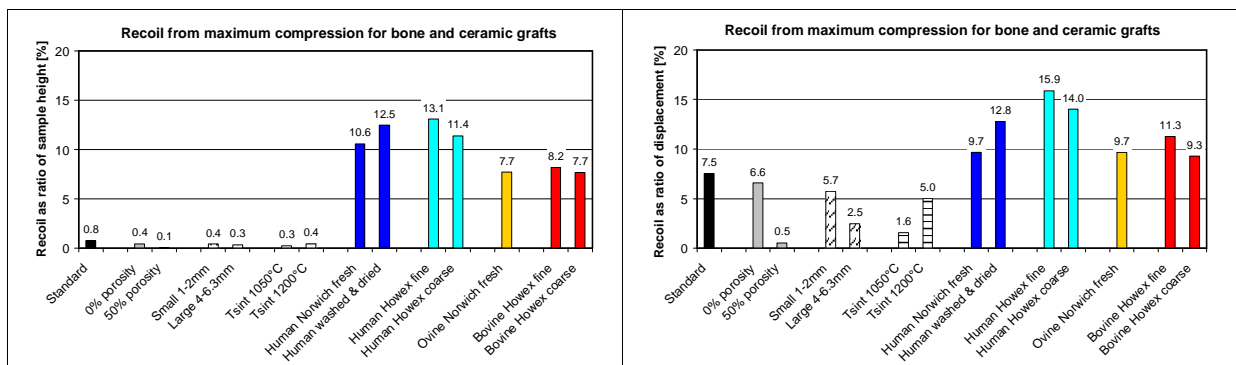


Figure 4.27: Recoil calculated for ceramic and bone grafts with relation to the sample height at maximum compression (left) and with relation to the displacement (right).

When the compressed ceramics were re-compressed for a second time and up to 1000N, twice the initial peak load, the force-strain responses followed the curves represented in figure 4.28. Similar to the observations for bone, during secondary compression the stress-strain curves ramped up steeply in a near linear way up to the 500N peak load of the initial compression (compare figure 4.17). The compression moduli during this phase were between 4.5 and 14.3 times higher than during the initial 0-500N compression depending on the ceramic configuration (see figure 4.30, table 4.4). At around 500N the stress-strain curves showed a distinctive change in slope and from ca. 600N onwards continued a near linear rise with R^2 -values between 0.89 (large 4-6.3mm particles) and 0.99 ($T_{Sint} = 1050^\circ\text{C}$ and standard ceramic). Even when the new, ca. 5-10% lower start height for was taken for the strain calculations, the increase in stiffness was only small (5-19%) for most ceramics. The original stress-strain relationship from the initial compression in principle continued once the initial peak load was exceeded. However, the high porosity (50%) and the low sintering temperature HA/TCP composite ceramics and the 68% porous pure HA ceramic continued compression with a 83% to 239% increased modulus (see also figure 4.30). This correlates to their low elastic recoil (figure 4.26) and indicates comparatively high levels of plastic deformation or crumbling.

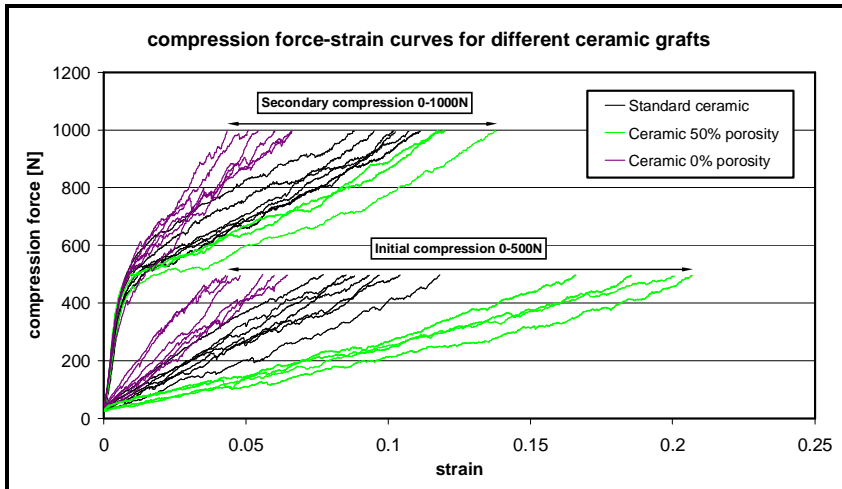


Figure 4.28:
Compression force vs. strain curves during secondary compression from 0-1000N for the standard ceramic and the stiffest and least stiff ceramic configuration.

Figure 4.29 compares the stress-strain responses of pre-compressed bone and ceramic grafts by displaying the graft configurations with the extreme moduli measured for the natural and synthetic grafts respectively. During the 0-500N compression phase, the pre-compressed ceramic grafts measured between 3.7 times (pure HA, 68% porosity) and 14.9 times ($T_{Sim}=1200^{\circ}\text{C}$) times higher compression moduli than the bone graft materials despite the fact that the pre-compression ratio for bone was higher and thus the new start height much lower than all ceramics (except pure HA material).

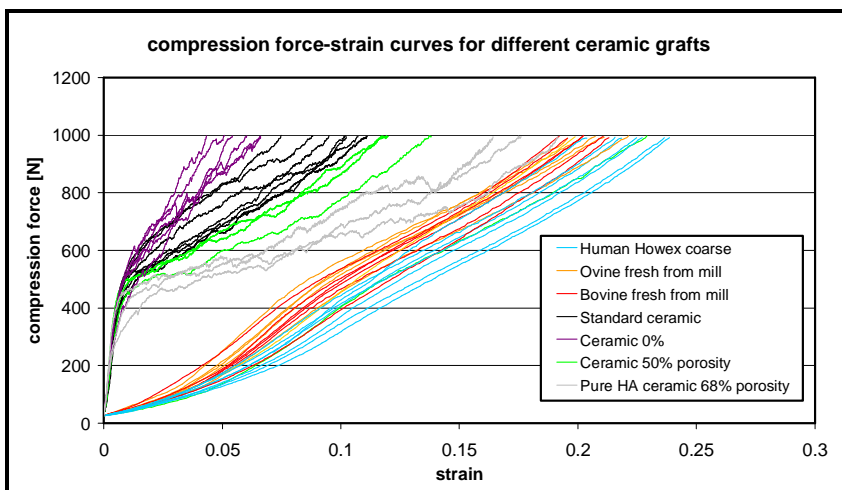


Figure 4.29:
Compression force vs. strain curves during secondary compression from 0-1000N for the stiffest and least stiff HA/TCP configuration, a highly porous HA and typical bone grafts.

Once the peak load of the initial compression went beyond 500N, both the bone and the ceramic graft showed a near linear stress-strain response with high R^2 -values between 0.89 and 0.99. During this phase, the slopes of the stress-strain curves, as the measure for compression modulus, were much closer for both bone and ceramic grafts than during the initial compression and the secondary loading to 500N. The minimum to maximum range measured from 12.5MPa (pure HA with 68% porosity) and 33.4MPa (0% porosity, see also table 4.4), a reduction in spread from 690% to 170%.

The increase in compression modulus between the initial 0-500N compression and the 0-500N and 500-1000N phases of the secondary compression are represented in figure 4.30 and table 4.4. The comparison reveals that the originally least stiff ceramics (high porosity, low sintering temperature, large particles) showed the highest modulus increase while the rise in stiffness of the high modulus ceramics remained low. As a result, the mechanical performance of different ceramic configurations became similar during re-compression and loading towards increasingly higher loads. For bone grafts, the stiffness increase during 0-500N re-compression was relatively low. However, as a result of the bones initially exponentially rising stress-strain curve, the highest modulus increase of all samples was measured when compression forces reached higher values. This effect brings into line the stress-strain responses of bone grafts with the ceramics both qualitatively and quantitatively. The differences in stiffness even became statistically insignificant ($p=0.099$) when the 50% porous HA/TCP ceramic (modulus=15.1MPa) was compared with Howex milled human (14.0MPa) and Norwich milled ovine graft (14.6MPa).

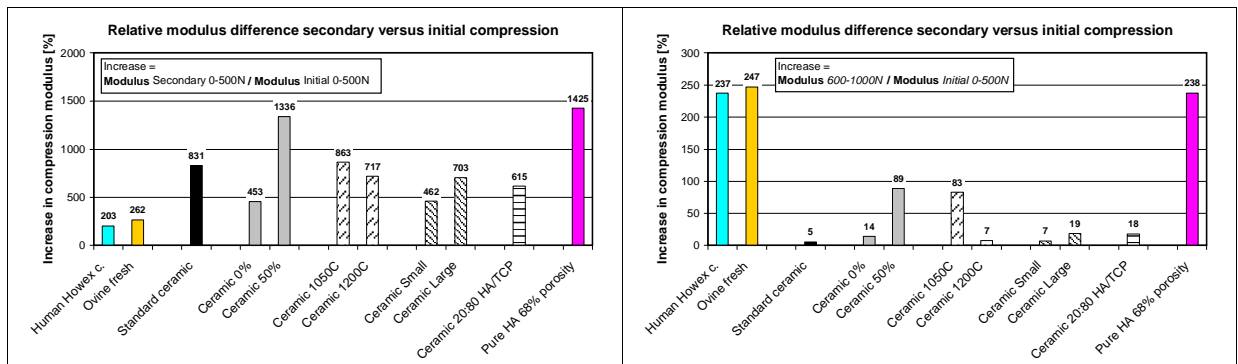


Figure 4.30: Relative modulus increase between the secondary 0-500N compression (left) or the 600-1000N compression phase (right) and the initial 0-500N compression.

The relaxation behaviour of granular ceramics after re-compression to a 1000N peak load was qualitatively identical to the observations made during relaxation from the initial 500N peak load and identical to the observations made for bone grafts. As shown in figure 4.31, this meant an exponential drop in reaction force once the crosshead was stopped and held in position. Quantitatively, relaxation was slightly less after re-compression measuring between 16.3% (50% porosity) and 17.8% ($T_{Sint}=1200^{\circ}\text{C}$) for the HA/TCP composite ceramic and 21.1% for the highly porous HA material (table 4.4). Relaxation of pre-compressed samples was on average 1.9 percentage points lower than after the initial 0-500N compression. Figure 4.31 illustrates this difference by superimposing the relaxation-time curves from the 500N and 1000N peak load for the standard ceramic after the peak force was normalised to 100%.

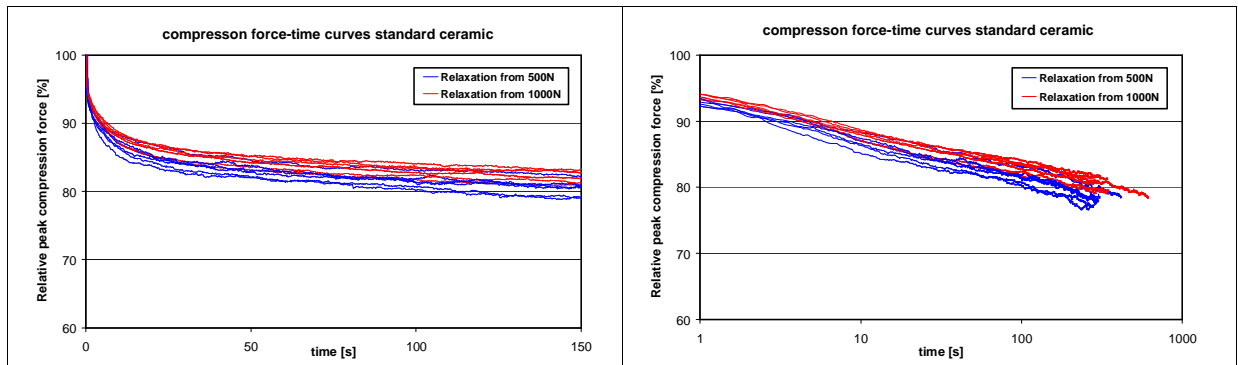


Figure 4.31: Superimposed relative relaxation versus time curves from 500N and 1000N for the standard ceramic. Peak force normalised to 100%, linear (left) and log-scale (right).

As pure ceramics are brittle materials, the particle size distribution after compression testing was determined. Granules were sieved and weighed into four different size classes after they had been loaded first to 500N and a second time to 1000N. Particle size ranges were chosen in accordance to the already defined size ranges small (1-2mm), medium (2-4mm) and large (4-6.3mm). Particles falling through the 1mm sieve were weighed to make the fourth “dust-like” class. The post-compression particle size distributions are graphically represented in figure 4.32 to figure 4.35.

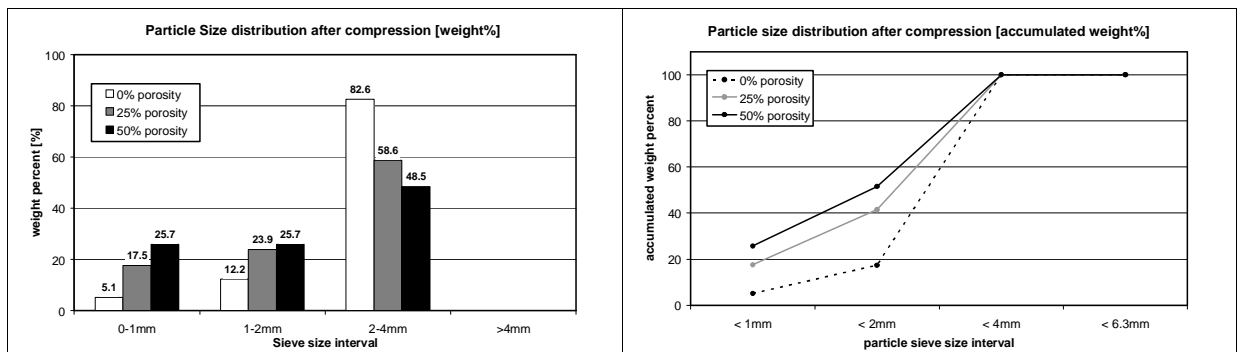


Figure 4.32: Particle size distribution after compression testing as weight% per size class (left) or accumulated weight-% below size class (right). Varied: Ceramic porosity.

Figure 4.32 shows that introducing porosity into a ceramic bone graft extender has a strong influence on the friability of the material under compression. After compression, 82.6 weight-% of the non-porous ceramics still fell into the original size category and only 6.1 weight-% were crushed to dust-like dimensions, the lowest proportion of all examined ceramics. That ratio changed strongly for the low 25% porosity samples where only 58.6% of the original weight was still in the original 2-4mm size class but 17.6% were fragmented to dimensions below 1mm. With 50% porosity the ceramic reached the second highest dust-like proportion of all HA/TCP grafts with more than one quarter (26.7%) of the original weight compressed to sub-mm granules. Less than half (48.5%) of the starting weight remained in the 2-4mm size

interval. The strong correlation between friability and porosity can be extrapolated with the highly porous pure HA ceramic (68% porosity) when the effect of chemical composition or sintering temperature is neglected. For this material the dust fraction after compression testing was nearly half the original weight measuring 43.6%. The minimum and maximum values for the dust weight fraction after compression were measured when the porosity was altered and this correlated with most properties described above like compression modulus, relaxation and recoil.

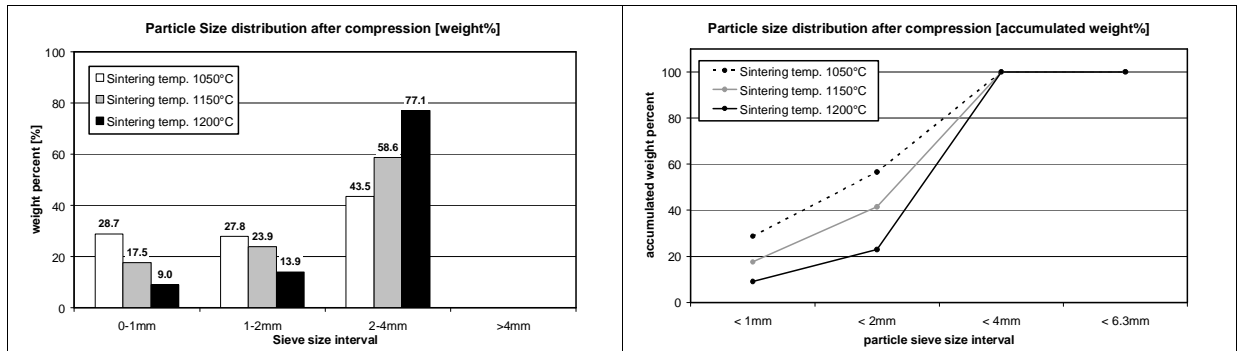


Figure 4.33: Particle size distribution after compression testing as weight% per size class (left) or accumulated weight-% below size class (right). Varied: Ceramic sintering temperature.

The influence of sintering temperature on the particle size distribution after compression testing is shown in figure 4.33. A high sintering temperature ensures a stable ceramic which contained 77.1 weight% in the original size interval after testing and produced only 9.0% dust. Samples sintered at lower temperatures did fracture significantly more with nearly identical weight percentages fracturing into the 1-2mm size category and values measuring 23.9% for $T_{Sint}=1150^{\circ}\text{C}$ and 27.8% for $T_{Sint}=1050^{\circ}\text{C}$. But ceramics sintered at the lowest temperature produced 28.7 weight-% of dust, nearly twice as much as the standard ceramic sintered at $T_{Sint}=1150^{\circ}\text{C}$ (17.6%). Again, the dust fractions correlate well with the weak performance of the low T_{Sint} ceramic during compression.

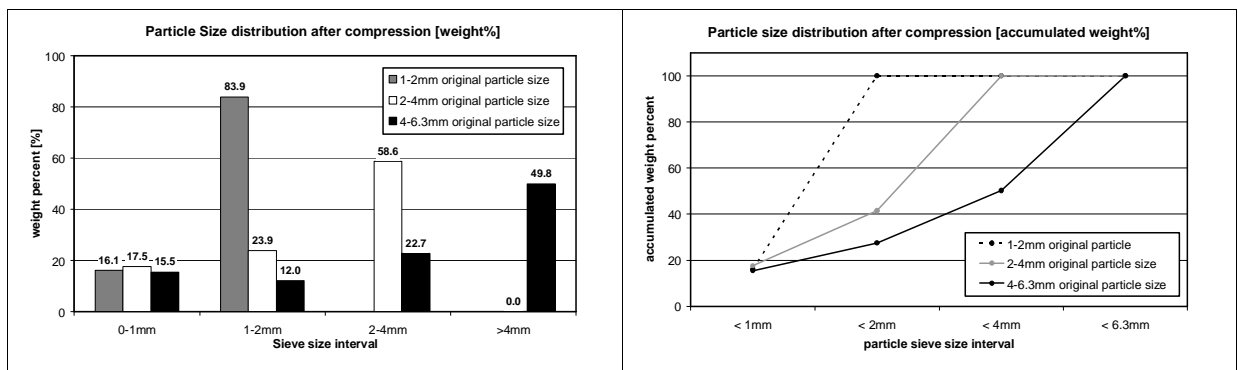


Figure 4.34: Particle size distribution after compression testing as weight-% per size class (left) or accumulated weight-% below size class (right). Varied: Particle size prior to testing.

When ceramic granules of different particle sizes were compressed, their post-compression size distributions showed an interesting commonality (figure 4.34). Independent of the initial particle size, the weight fraction of sub-mm particles after compression was nearly identical for all samples ranging between 16.1% (1-2mm original particle size) to 17.6% (2-4mm).

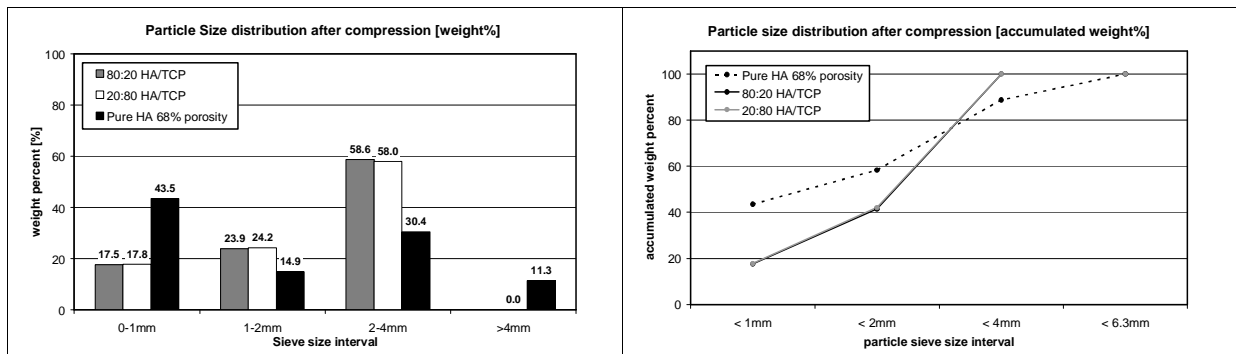


Figure 4.35: Particle size distribution after compression testing as weight-% per size class (left) or accumulated weight-% below size class (right). Varied ceramic chemical composition.

Reversing the chemical composition of the standard ceramic from 80:20 HA/TCP to 20:80 HA/TCP had no significant effect on the particle size distribution after compression (figure 4.35). The line graphs for both sample groups can hardly be distinguished. The pure HA sample included in the graph showed the highest dust weight fraction but, as described above, this effect must be the result of the 68% porosity level, the highest tested and much higher than the 25% porosity present on the ceramic configurations of the graph.

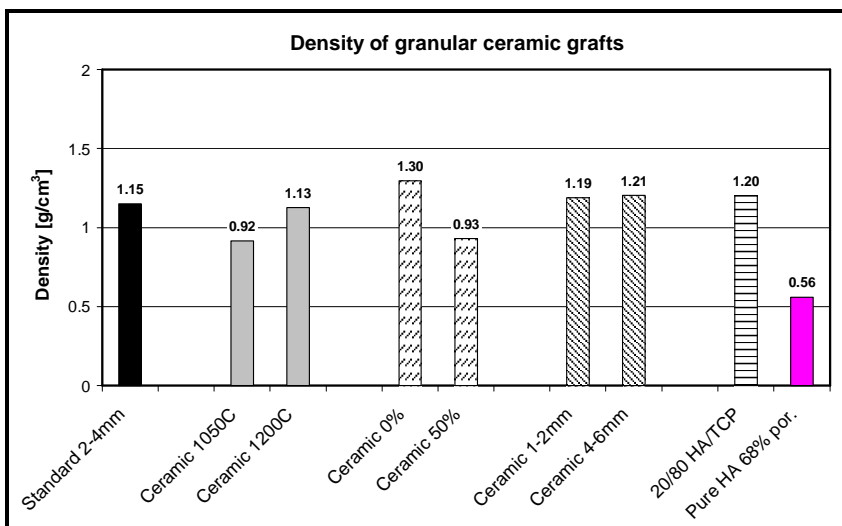


Figure 4.36: Density of loosely packed granular ceramics designed as bone graft extenders.

The extreme difference of the pure HA sample in comparison to the HA/TCP composites is further underlined by the density measurements of the uncompressed bulk material as given in figure 4.36. The highly porous pure HA recorded an average density ρ of 0.56 g/cm³, a value

nearly 40% lower than measured for the HA/TCP composite ceramic with the lowest density of 0.92 g/cm^3 ($T_{\text{Sint}} = 1050^\circ\text{C}$). Again porosity had the biggest influence on materials' properties with the maximum density of 1.30 g/cm^3 recorded for the non-porous ceramic. Despite different packing efficiencies to be expected from differently sized ceramics, the densities of bulk loosely packed small, medium and large granules were nearly identical.

4.4.3 Results - bone graft and ceramic mixes

The compression behaviour of graft mixes of bone and granular ceramics as bone graft extenders is documented below. The standard configuration ceramic, a 80:20 HA/TCP ceramic with 25% porosity, sintered at $T_{\text{Sint}} = 1150^\circ\text{C}$ and with medium sized 2-4mm particles was mixed with fixed ovine bone graft in three different volumetric mixing ratios of 2:1 bone/ceramic (b/c), 1:1 b/c and 1:2 b/c. Figure 4.37 shows one typical compression-force time curve measured for a 1:1 bone/ceramic graft mix during the initial 0-500N compression test. Such a graph was also produced for both mixing components, pure bone graft (figure 4.4) and pure ceramic (figure 4.19) and when compared to each other, one can see how characteristic features of the two components combined to create a distinctive stress-strain and relaxation behaviour for a bone/ceramic mix influenced by its components (also figure 4.38).

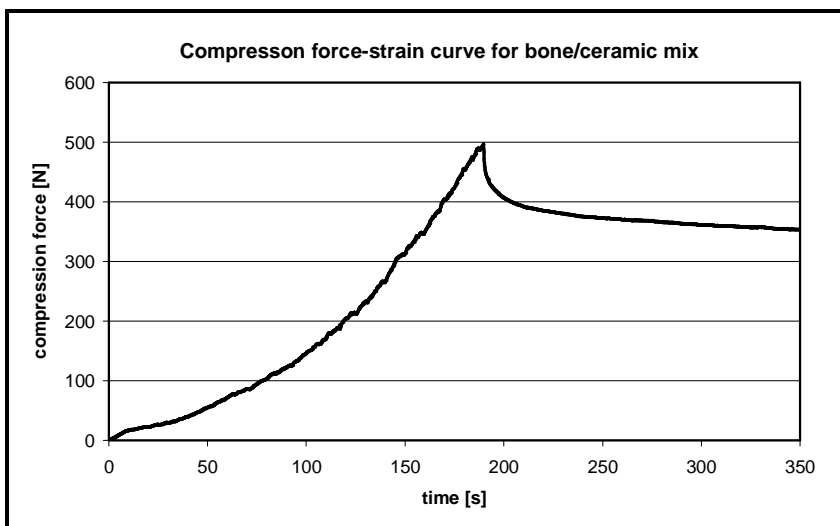


Figure 4.37:

Typical compression force vs. time curve for a 1:1 volumetric bone plus ceramic graft mix.

As shown in figure 4.37, the bone/ceramic mix produced a stress-strain curve exponentially rising to the peak load, a typical behaviour observed for bone grafts. However, the exponent of this relationship was lower for the graft mixes and decreased when the ceramic fraction was raised (figure 4.38). Also typical for the stress-strain curves of graft mixes is a saw-tooth

profile superimposed on the exponential trend, a feature introduced by the ceramic content. It becomes more pronounced when the ceramic fraction is increased. Figure 4.38 compares the stress-strain curves of the 2:1, 1:1 and 1:2 bone/ceramic mixes with the compression performance of its pure constituents, fixed ovine bone graft and the standard ceramic. The stress-strain curves for the mixing components and the graft mixes are clearly separated documenting a distinctive graft performance. The exponential compression behaviour of bone and the typical saw-tooth profile created by the ceramic particles combine in intensity according to the mixing ratio. The stress-strain curves of all b/c mixes were shifted more towards the compression response measured for pure bone than for ceramic. Even the 1:2 b/c mix showed a dominant influence of the bone graft phase indicating that already relatively small amounts of bone graft strongly affect the mechanical performance of graft mixes.

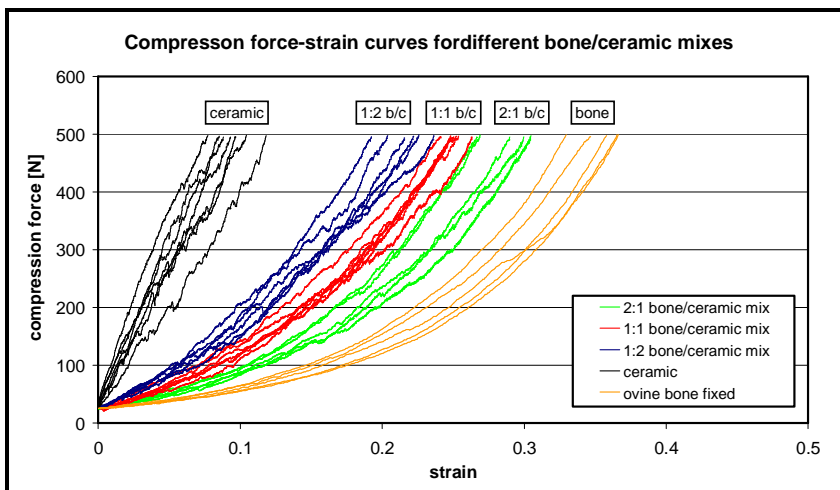


Figure 4.38:

Compression force vs. time curves for different volume mixes of bone graft with the standard ceramic extender compared to pure bone and pure ceramic for reference.

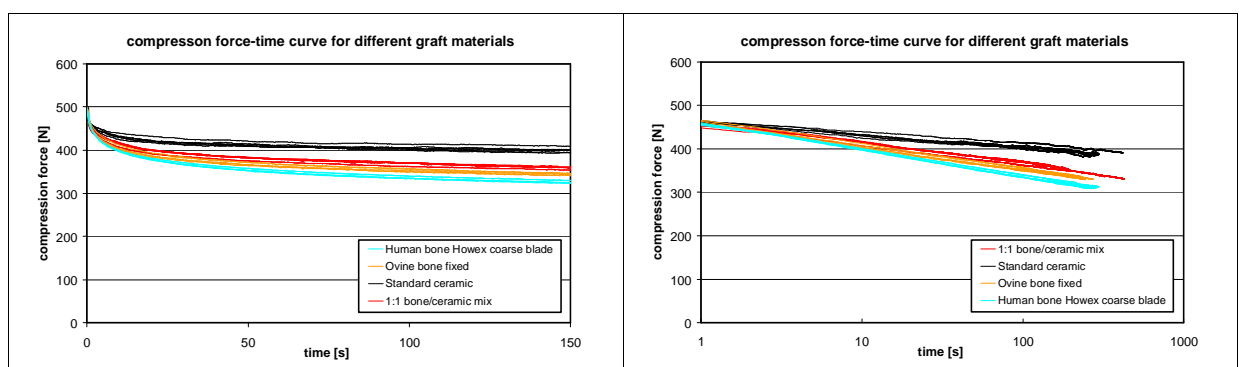


Figure 4.39: *Time-relaxation curves for a 1:1 b/c mix compared to its pure constituents, ovine bone plus ceramic and human bone. Left: linear time scale, Right: logarithmic time scale.*

As relaxation for pure bone grafts and pure ceramic extenders was qualitatively identical and only differed in intensity, the relaxation behaviour of the bone/ceramic mixes also followed this exponential drop in reaction force. As figure 4.39 shows for a 1:1 b/c mix as an example, the relaxation level lay clearly separated in-between the performance of the mixing phases.

Again, as with regards to the stress-strain response, the relaxation behaviour of the b/c mixes was closer to that of the bone graft phase than that of the ceramic extender.

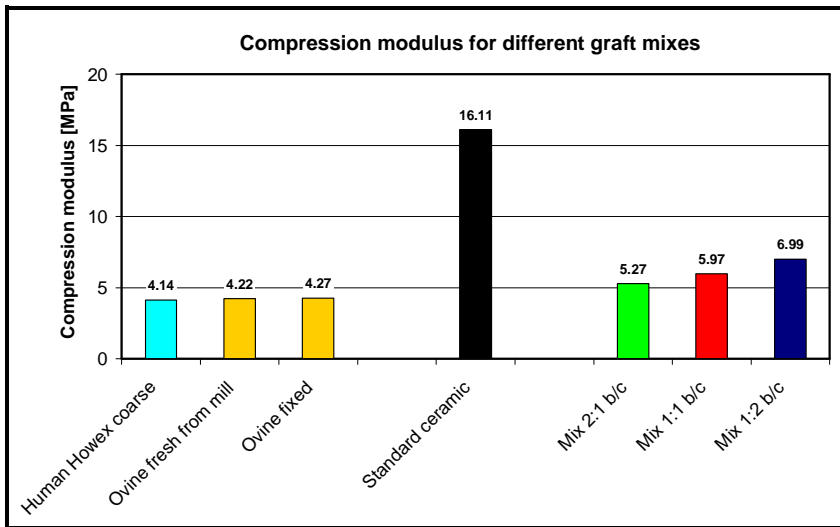


Figure 4.40:

Compression moduli for different mixes of fixed ovine bone and the standard ceramic graft during the initial 0-500N compression.

Figure 4.40 and table 4.5 quantify the observations made in figure 4.38 by using a bar chart to display the secant compression moduli calculated during the initial 0-500N loading. The lowest average modulus was calculated for the high bone content 2:1 b/c mix (5.27MPa), the highest for the high ceramic content 1:2 b/c mix (6.99MPa) with the equally composed 1:1 bone/ceramic mix lying in-between with a stiffness value of 5.97MPa.

As qualitatively described above, the b/c mixes assimilated more the performance of the bone graft phase in the mix. Even the stiffness of the high ceramic content 1:2 b/c mix was much closer to the modulus of fixed ovine bone (4.27MPa) than to its dominant ceramic phase (16.11MPa). The dominant influence of the bone graft properties in the mix is also reflected in the relatively small influence the ceramic had on the stiffness levels of different mixing ratios. The spread of minimum to maximum modulus for different mixes was only 33%, lower than the modulus spread calculated for all bone grafts tested (35%).

A similar situation was observed during relaxation from the initial 500N peak load. As shown in figure 4.41 and table 4.5, relaxation for the bone/ceramic mixes ranged between 26.7% (1:2 b/c) to 27.5% (1:1 b/c) and thus was much closer to the relaxation measured for fixed ovine graft (30.1%) than for the pure ceramic (18.7%). The differences between relaxation values measured for the different mixing ratios were statistically not significant ($0.05 < p < 0.70$). The spread of relaxation values measured for differently prepared human grafts (32.4% to 38.5%, figure 4.15) was larger than for b/c mixes of different composition ratios.

GRAFT MATERIAL	Modulus									Relaxation		Recoil
	1. comp. 0-500N	SD	SD	2. comp. 0-500N	SD	SD	2. comp. 0.5-1kN	SD	SD	from 500N	from 1kN	from 500N
	[MPa]	[MPa]	[%]	[MPa]	[MPa]	[%]	[MPa]	[MPa]	[%]	[%]	[%]	[%]
Human Howex coarse	4.14	0.08	1.9	12.54	1.12	9.0	13.98	0.93	6.6	33.1	32.7	11.4
Ovine fresh from mill	4.22	0.07	1.7	15.29	1.73	11	14.63	0.81	5.5	39.6	40.7	7.7
Standard ceramics	16.11	2.17	14	149.9	31.9	21	17.0	0.3	2	18.7	17.3	0.77
2:1 bone/ceramic mix	5.27	0.33	6.2	19.4	2.70	14	16.1	1.37	8.5	27.2	27.6	7.3
1:1 bone/ceramic mix	5.97	0.18	2.9	23.9	1.53	6.4	17.6	0.40	2.3	27.5	27.4	5.0
1:2 bone/ceramic mix	6.99	0.52	7.4	31.2	3.99	13	16.4	0.98	6.0	26.7	26.2	3.1

Table 4.5: Secant compression moduli, relaxation and recoil values for various bone/ceramic mixes.

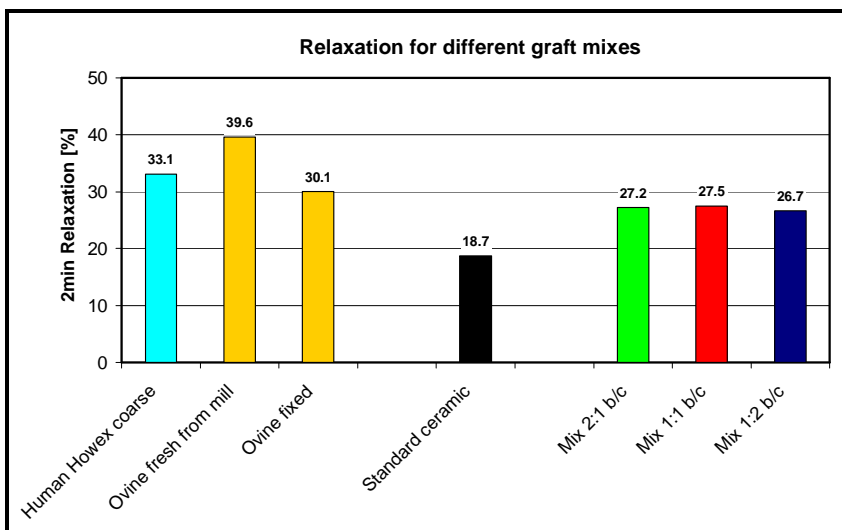


Figure 4.41: Relaxation for different mixes of fixed ovine bone and the standard ceramic graft during the initial 0-500N compression.

Also recoil behaviour showed that the properties of bone/ceramic mixes are predominantly affected by the bony phase in the mix. As figure 4.42 shows for both previously defined recoil calculations, recoil for graft mix ranging from 3.1% for the 1:2 b/c mix to 7.3% for the 2:1 b/c mix were much closer to the 7.7% of recoil recorded for the ovine bone phase than the 0.8% measured for the ceramic component in the mix.

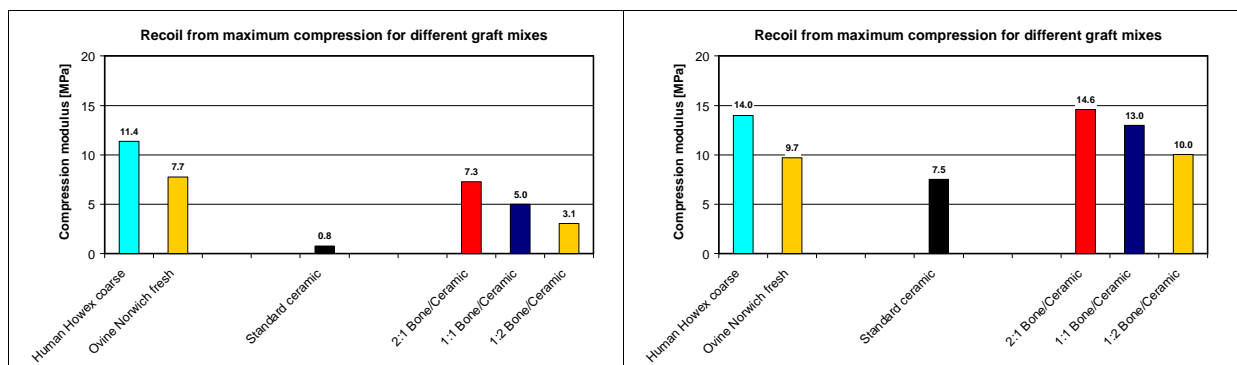


Figure 4.42: Recoil calculated for bone/ceramic graft mixes with relation to the sample height at maximum compression (left) and with relation to the maximum displacement (right).

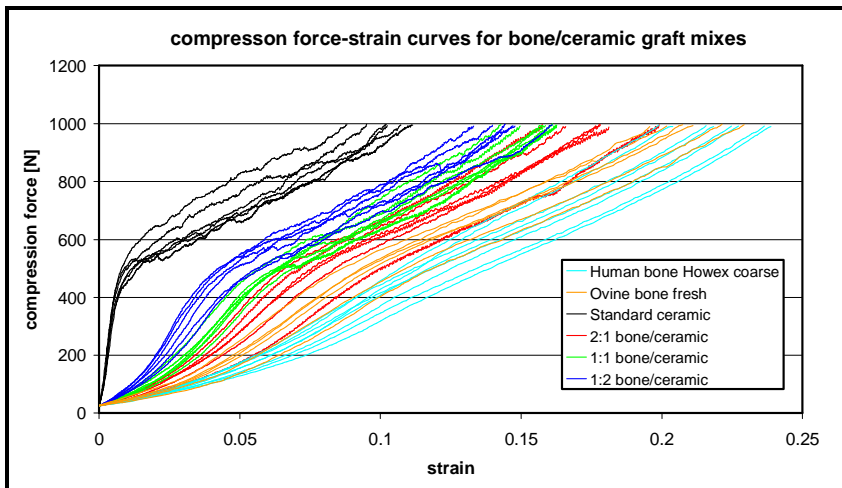


Figure 4.43: Force-strain curves for different bone/ceramic mixes during secondary compression from 0-1000N in comparison to the pure ceramic and typical bone grafts.

Secondary re-compression to a peak load of 1000N confirmed the above observations about the closer similarity of bone/ceramic mixes with pure bone than pure ceramic. At the same time, the trend that differences between pure bone and ceramic configurations were reduced when compressed towards higher forces was also noticeable for the graft mixes. Figure 4.43 displays the stress-strain curves of the graft mixes during secondary compression and compares them to the performance of both pure phases. When compared to figure 4.35 (initial compression), it can be seen that the stress-strain curves for the graft mixes were even closer to the stress-strain response of bone and at the same time closer to each other than before.

Quantitative analysis of this observation is documented in table 4.5 and figure 4.44. As shown before for pure bone and ceramic, grafts with initially low moduli showed a significantly higher increase in modulus during high force compression than initially stiffer materials. With a stiffness increase of 247% for ovine bone, 5% for the pure ceramic and between 135% and 206% for the mixes, moduli during re-compression from 500-1000N were almost identical for these graft materials ranging from 14.6MPa (ovine bone) to 17.6 MPa (1:1 b/c mix) only.

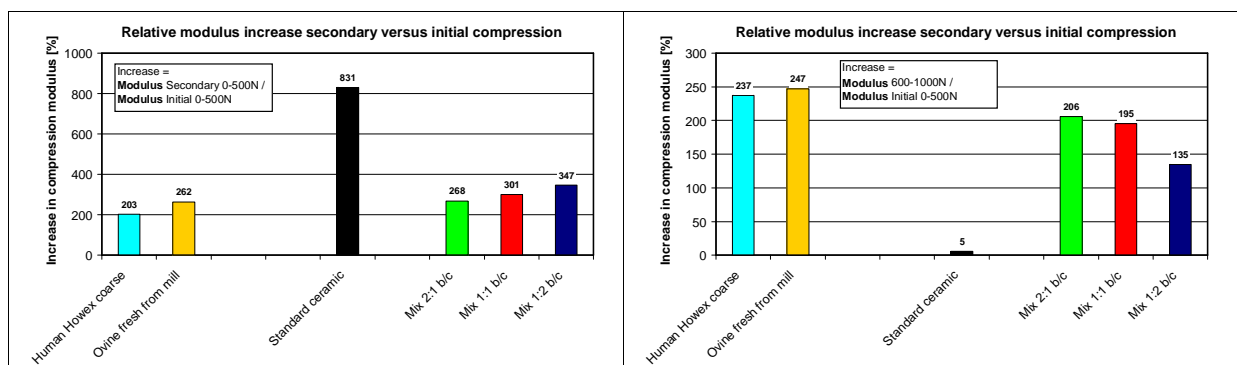


Figure 4.44: Relative modulus increase between the secondary 0-500N compression (left) or the 600-1000N compression phase (right) and the initial 0-500N compression.

The relaxation of bone/ceramic mixes from high compression loads (table 4.5) also followed the same trend already observed for the pure bone and ceramics grafts. Relaxation of pre-compressed samples re-loaded to a higher peak load of 1000N was only slightly less than measured after the initial compression. Table 4.6 summarises results.

- **Qualitative compression properties of all bone grafts**
 - Exponential stress-strain response during initial compression to 500N.
 - Linear stress-strain response during re-compression and compression towards high loads.
 - Exponential relaxation.
 - Stiffness increase during re-compression.
- **Effects of graft preparation, storage, sterilisation**
 - Stiffness*
 - Bone mill type has significant influence on stiffness (Howex: higher modulus, lower variability; Norwich: lower stiffness, higher variability) No influence of blade type.
 - Other treatments (washing & drying, fixation or high level irradiation) - no significant effect on stiffness.
 - Relaxation*
 - High variability – not many significant differences.
 - Fixed (and washed and dried) ovine graft not significantly different to fresh human graft.
 - Relaxation of human and xenografts bone similar.
 - Washing and drying and fixing affected relaxation of ovine bone but not human bone.
 - Recoil*
 - No significant difference between human bone grafts. Recoil of xenografts lower than human bone but significant only in comparison to Howex milled human graft.
 - Modulus differences during initial compression reduced during re-compression and towards higher loads.
- **Ceramic bone substitutes**
 - Linear stress-strain response with superimposed saw-tooth profile.
 - Relaxation qualitatively identical to bone but lower.
 - Stiffness much higher than bone and highly variable depending on configuration.
 - Only the highly porous HA tested for comparison had a lower modulus than bone.
 - Relaxation of all HA/TCP configurations identical (no significant differences).
 - Porosity most sensitive property. Increasing porosity massively reduces modulus.
 - Also sintering temp. ($T_{\text{Sint}} \downarrow = \text{stiffness} \downarrow$) and size (size $\uparrow = \text{stiffness} \downarrow$) affect stiffness, no effect of composition.
 - Recoil of different configurations not correlated with relaxation (constant) but stiffness.
 - During re-compression and loading towards higher forces, modulus ranking of ceramic configurations remained the same but differences decreased. Strong assimilation of stiffness within ceramics group and between ceramics and bone.
 - Dust weight fractions correlate well with stiffness. Ceramic density suitable indicator.
- **Mixes**
 - Bone/ceramic mixes combine properties of constituents according to mixing ratio.
 - Influence of bone graft phase dominant for compression, relaxation and recoil.
 - During re-compression to high loads, compression properties assimilate between mixes and in comparison to bone and ceramic. The properties of different mixes become statistically indistinguishable.

Table 4.6: Summary of results from compression testing of bone, ceramic and graft mixes.

4.5 Discussion

4.5.1 Discussion - bone grafts

At low compression forces up to 500N, all human bone grafts and xenografts showed an exponential stress-strain response as represented in figure 4.4 (human bone) or figure 4.11 (xenograft bone). Further compression of pre-compressed samples to higher loads up to 1000N led to near linear stress-strain relationships ($R^2 > 0.99$) for loads exceeding the original 500N peak for all bone grafts as shown in figure 4.5 or 4.8 for human and figure 4.17 for xenograft bone.

This qualitative behaviour is the result of the multiphase composition of bone graft and the constrained nature of the die-plunger test. Apart from the mechanically stiff mineral bone phase found as granules of trabecular bone, the morsellised grafts are wet containing liquids in the form of blood, water or residual fixative and a high volume fraction of viscoelastic organic material such as fat, collagen or cartilage. During initial compression to the lower 500N peak load when strain maxima of approximately 0.5 were reached, the liquids were squeezed out of the sample through the porous disk introducing a viscoelastic stress-strain response similar to that of a viscous damper. The organic phase, viscoelastic in nature and thus not giving Hookean linear stress-strain responses, also contributes to the non-linear exponential stress-strain curves measured for the bone grafts. When the compression force during the secondary compression phase exceeded the initial peak force and when maximum strain levels reached values in excess of 0.6, the stiff and hard particles of trabecular bone increasingly come into contact with each other so that the load bearing characteristics shift from the organic matrix of the sample and from squeezing out liquid to the stiff bone mineral phase. As a consequence the stress-strain response is, like for the ceramic grafts, nearly linear during this stage. In addition, the sample's containment as a result of the die-plunger set-up constrains lateral expansion and thus contributes to the compression performance at higher loads and strains. In theory the stress-strain response of such constrained samples would become exponential again at loads even higher than those tested.

The effect of viscoelasticity causing strain-rate dependent stress-strain responses and the great effect of wetness or liquid content of bone grafts on the mechanical response during laterally constrained compression is highlighted in figure 4.6. When a low liquid penetration rate is only possible through the die-plunger gap, the stress-strain curves at the relatively high strain rate of 3mm/min showed sudden steep rises in reaction force with a huge margin of tolerance for the peak strains recorded. Lowering the strain rate to one tenth at 0.3mm/min resulted in a

stress-strain response more similar to towel dried bone or wet bone during compression with a highly porous plunger. Towel dried bone and wet bone compressed with a plunger allowing high liquid penetration rates at low resistance showed nearly equal stress-strain responses. The towel dried bone was slightly stiffer correlating with the fact that towel dried bone still contains residual wetness which must be squeezed out at higher loads. This introduces additional viscoelasticity and a more pronounced exponential stress-strain rise. However the relative similarity of nearly dry bone and wet bone compressed with a porous plunger proves that the high permeability chosen for the porous plunger was sufficient to minimise the described negative effects that compressing incompressible liquids unable to escape can have on the stress-strain behaviour of bone grafts.

The viscoelastic nature of bone grafts is also reflected in the relaxation behaviour of the samples as shown in figure 4.13 and 4.14 (relaxation from initial 0-500N compression) and figure 4.18 (relaxation from secondary 0-1000N compression). In all cases for human and xenograft bone, the reaction force decreased exponentially once compression was stopped and the plunger held in the position of maximum strain. On a logarithmic scale the force-time curves were linear in good approximation even when the relaxation time was increased to a value nearly tenfold the standard period of $t=120$ s as shown in figure 4.13. Thus taking relaxation measurements as a relative drop in reaction force after a 2min period gave a sufficiently characteristic indicator of differences between graft relaxation behaviour.

Figure 4.7 and figure 4.8 show two sets of stress-strain curves belonging to two types of human bone graft which gave the lowest (Norwich milled graft) and highest stiffness (Howex coarse blade milled graft) of all human grafts. It indicates that of all preparation and storage methods of human bone graft tested, the bone mill type has the strongest influence on stiffness. Howex milled graft (both blade types) was not only significantly stiffer but also less variable than Norwich milled bone. Other preparation or storage methods apart from bone mill type did not have a strong effect on bone graft stiffness, neither drying, washing and drying, multiple freeze thaw cycles or formalin fixation nor different levels of γ -irradiation. This observation confirms the earlier finding that graft stiffness is dominated by the quality of the trabecular bone particles and not by organic phase or liquid content (blood, water, fixative residuals) which are mostly affected by such treatments.

The choice of bone mill type with their different operating principles and blade types mainly affects size, size distribution and morphology of the trabecular bone graft particles. Liquid content and volume fraction of the organic phase are unaffected. This is the opposite with the other bone graft preparation and storage methods. Drying, washing and drying, multiple freeze thaw cycles or formalin fixation and different levels of γ -irradiation do not affect much

the mineral phase of bone and thus an effect on the stiffness of morsellised bone grafts is less expected. However they change the presence or properties of the organic phase. Drying, washing and drying, multiple freeze thaw cycles, formalin fixation for instance alter the liquid content and thus the materials' viscoelasticity. Formalin fixation and γ -irradiation affect the viscoelastic properties of the organic phase by cross-linking the polymeric materials. As viscoelasticity influences the relaxation behaviour, different relaxation levels are expected and in fact were observed for human bone grafts treated in such ways. At the same time, no significant difference in relaxation was measured for the two different bone mills.

The hypothesis that bone graft stiffness is mainly affected by the trabecular phase and that relaxation is mainly affected by liquid content and the volume fraction of the organic phase is further supported when the compression test results of the xenografts are included in the comparison. Both ovine grafts and bovine grafts are significantly stiffer than the fresh Norwich milled human graft as shown for instance in figure 4.11. and 4.12 or table 4.3. Bone from different species has a different trabecular structure and density and a different volume ratio between trabecular and cortical bone. The cancellous bone of a bovine femoral or humeral head is so dense that it cannot be milled with a Norwich mill but by the more stable and crude Howex bone mill only. The ovine humeral heads for instance are much smaller in overall diameter so that, by geometric considerations alone, it becomes obvious that a different ratio of cancellous to cortical bone will be present in morsellised ovine graft than human graft. Despite removal of obvious cortical bone chips and despite similar visual appearance, morsellised ovine bone will contain a higher volume fraction of stiff cortical bone than human graft. As a result the measured moduli were higher.

The different stiffness of ovine graft to Norwich milled human graft is nearly identical to the increase achieved for human bone by using the Howex mill. As a result, the moduli of ovine grafts and the Howex milled human grafts are nearly identical during both the initial 0-500N and the secondary 0-1000N compression (table 4.1). Bovine bone however is significantly stiffer.

Comparing the standard deviations of the stiffness measurements for the human and xenografts identifies that the Norwich milled human grafts score much higher variability with $3.0\% \leq \sigma \leq 5.4\%$ than the Howex milled human grafts with $1.7\% \leq \sigma \leq 1.8\%$ and the ovine and bovine xenografts with a standard deviation range of $1.7\% \leq \sigma \leq 4.5\%$. As expected, the stiffness properties of human bone graft are more variable than ovine graft prepared with the same mill because of the differences in bone sourcing. Human bone graft is harvested from individual donors of various size, sex, age, health resulting in an enormous range of bone properties easily identifiable even by superficial visual inspection (figure 3.1). The ovine bone graft however is sourced from a butcher who uses sheep of comparably constant size and a

young age guaranteeing a constant healthy bone condition. The higher variability of human bone versus ovine xenograft is so large that it was identified despite mixing the human bone graft from up to 10 femoral heads in order to level out the inconsistencies between individual heads, a quantity significantly higher than the 1-3 human femoral usually morsellised and mixed during clinical impaction grafting.

The variability of human graft's compression stiffness was reduced when the Howex mill instead of the Norwich mill was used for morsellising bone chips. This correlates well with the comparison of the visual appearance of the bone chips produced by both mills. The Howex milled bone chips looked much more consistent in size and shape than the Norwich milled graft. In particular, very large individual bone chips exceeding 10mm in size were absent. The Norwich milled graft appeared less consistent in size and shape and contained a number of large bone fragments which had to be cut down manually using a pair of cutters. The outcome also was dependent on the rotational speed of the blade and the feed pressure.

The differences in mill performance are the result of the design and the type of blade action. The solidly built Howex mill is very stiff and guarantees a constant gap between feeder tube and the maximum diameter of the blade drum. The Norwich mill has a feeder tube where the distance to the rotating drum is adjustable transferring responsibility for the ideal set-up from designer to user. At the same time the dimensions of the components are too weak to withstand substantial elastic deformation which alters the relative position of drum and feeder to each other, a measurement highly critical for morsellising the bone. High torque and feed pressure are frequently required to overcome blockage of the mill. This can lead to contact of the feeder tube and the drum blunting the blades and interrupting the milling process. On the contrary, the spring-like elastic recovery can open up the gap between feeder and drum. Bone fragments can get caught between the surfaces wedging open the space even further. As a result large pieces of bone with maximum dimensions of up to 30mm can escape the milling process and fall into the tray. This effect is worsened by the lack of a full enclosure of the blade drum like it is found on the Howex mill. In combination with the constantly tight feeder/drum gap, such an enclosure guarantees that all graft is morsellised by the blades and does not escape around the circumference. The spacing between the straight blades of the Howex mill is much wider than that between the many circular blades of the Norwich mill. This aides a smoother operation of the mill as it hardly gets blocked and requires less feeder pressure. With its protruding hook-like blades, the Howex mill grips and positions the femoral heads much better and consistently than the Norwich mill as well. The sturdiness and superior blade design of the Howex mill also enables it to morsellise the very dense bovine trabecular bone, a task the Norwich mill fails to do.

Relaxation of the ovine and bovine xenografts lay within the bandwidth measured for the human bone grafts (fig. 4.14 and fig. 4.15). This indicates that the condition and quantity of organic material is similar to human bone. For instance washed and dried ovine bone and Howex milled human bone do not show any statistically significant difference in relaxation. However, pure ovine bone scored the highest relaxation of all bone samples and was most strongly affected by washing and drying or fixation resulting in the lowest relaxation values of all bone grafts. This indicates that fresh ovine bone graft contains a relatively high fraction of organic material which when removed by washing & drying or when crosslinked by formalin fixation changes viscoelasticity significantly.

Relaxation after the secondary compression to 1000N scored was only marginally less than relaxation after the initial 0-500N compression (table 4.2). This indicates that even after the 1000N loading regime the mineral and organic phases have sustained their viscoelasticity and are not heavily damaged so that a near identical relaxation pattern can occur. It also proves that characterising relaxation by a giving a percentage drop in reaction force is a relevant characteristic property.

4.5.2 Discussion - ceramic graft extenders

The stress-strain responses of the pure ceramic bone graft extenders were entirely different from human and xenograft bone both qualitatively and quantitatively. As shown in fig. 4.19 and 4.21 ceramics compress with a linear stress-strain relationship superimposed by a saw-tooth profile. For most ceramic configurations this linear stress-strain relationship continued when pre-compressed samples were reloaded and compressed up to 1000N as shown in fig. 4.25 or 4.28. No exponential stress-strain rise like that observed for bone was noticed. This indicates that up to the peak stress of 3.18MPa, the mechanical response of ceramics is governed by elastic Hookean behaviour. Ceramics from the standard configuration provided by TCM Associates, U.K. were all much stiffer than the human and xenograft bone chips.

The slope of the stress-strain curves and thus the stiffness moduli vary with the ceramic's configurations and can be altered widely as show in fig. 4.22. The saw-tooth profile superimposed on the linear trend of the stress-strain curves is the result of fracturing granules. The higher the porosity, the more stress-risers are present in the granules and the more of these fractures can be observed. Due to the random nature of these fractures and the significant drop in reaction force they cause, the variability in stiffness recorded for pure ceramic bone graft extenders ($10.2\% \leq \sigma \leq 16.7\%$) was larger than for bone although ceramics are produced in a highly consistent manner.

The stiffness of ceramic graft extenders can be altered in a very broad range when the production parameters are varied. The effects of porosity levels, particle sizes, sintering temperatures and chemical composition on stiffness are shown in fig. 4.23. The ceramic properties are most sensitive to changes in the porosity levels. Both the highest and the lowest stiffness were recorded for samples with the lowest and the highest porosity respectively. Porosity introduces stress concentrations in the material so that fracture and collapse of the granules contribute massively to the stress-strain performance of the material. When the pure HA material with its 68% interconnected porosity is taken into consideration, the range of stiffness for the production of ceramic graft extender measures nearly 700% and it can even be below the stiffness of human bone graft.

Also sintering temperature (113% stiffness range), particle size (69.7%) and chemical composition (11.7%) allow manipulation of the stress-strain properties of ceramic graft extenders. Sintering temperature is known to affect the hardness and friability of the bulk ceramic by affecting phase changes and crystallinity and thus has a strong effect on stiffness during compression.

The influence of particle size on stiffness is a consequence of geometrical and load transfer considerations of particles compressed in a constrained volume with similar dimensions between granules and die. With a minimum to maximum size range of particle dimensions from 1mm to 6.3mm, the ratio between the die diameter and the particle sizes ranges from only 3.2 to 20. This does neither allow efficient packing to the theoretical maximum density nor does it allow a homogenous, quasi-continuous (indiscrete) load transfer. Therefore particle size must affect the mechanical performance of a granular material compressed in such volumetrically constrained conditions. The smaller the particles the more contact points exist between the granules themselves and with die-plunger. The load transfer is distributed over a larger amount of contact points and granules reducing stresses and fractures. At the same time packing is higher so that more ceramic material is active during load transfer. Thus the highest stiffness is recorded for the small sized particles.

The opposite effect is true for the large particles. Efficient, homogenous and reproducible packing of the large 4-6.3mm granules is not possible in a hollow cylinder of only 10mm radius. Load applied by the plunger is transmitted only via a few granules which themselves are supported only by a low number of contact points creating large voids within the aggregate. This way high contact stresses cause particle fracture and collapse of the fragments into the voids resulting in high strains and low stiffness values. As the conditions of packing

large particles are less reproducible than with the small granules, the standard deviation measured for the 4-6.3mm particles (14.6%) was higher than for the 1-2mm particles (11.2%).

Reversing the chemical composition of the standard 80:20 HA/TCP composite to an 20:80 HA/TCP composition had no statistically significant influence on the stiffness of the granular ceramic graft ($p= 0.231$). Composition ratios express the weight ratios of the powder components prior to mixing and sintering. Both the HA and TCP undergo phase transitions during sintering so that the final composite is of different composition than the powder mixing ratios and the different mechanical properties of the pure components confirm that this is the case. Additionally, the influence of porosity, granule size and shape, sintering temperature and sample packing is more dominant than chemical composition obscuring potential differences of the bulk material.

The described relative stiffness rankings are sustained when the pre-compressed ceramic samples are re-loaded to a higher peak force (table 4.4). However, ceramics of originally low modulus, like the highly friable ceramics of high porosity (50% HA/TCP and 68% HA) and low sintering temperature ($T_{Sint}=1050^{\circ}\text{C}$), recorded significantly increased moduli. As a consequence the mechanical performance of the initially very different ceramic configurations is assimilating. This behaviour is the result of the high rate of particle fractures and granule collapse of the less stiff and more friable ceramics during initial loading. It stiffens the aggregate by filling destabilising voids in the packing arrangement and by creating more contact points for load transfer reducing stress peaks. When particles fracture, the size range of the compressed grafts widens and allows improved packing efficiency approaching a theoretical ideal^[206]. Additionally, the many small, dust-like particles created during fracturing have dimensions below or near pore size and thus are by porosity weakening larger granules. Less stiff and friable ceramics thus have a kind of “self-stiffening” effect during compression.

The explanation of the self-stiffening effect at higher loads with the increased production of small dust-like particles due to fracture and breakage is supported by the comparison of particle size distributions measured prior and post compression testing (fig. 4.32 to 4.35). The ceramic configurations with the highest stiffness increase, the 50% porosity HA/TCP, the 68% porous HA and the HA/TCP sintered at 1050°C were the most friable ones, producing greater weight fractions of sub 1mm particles than their stiffer counterparts. For most samples, the higher the stiffness increase, the higher was the dust volume fraction produced. At the same time, the HA/TCP particles with reversed composition which possessed near equal stiffness values produced identical particle size distributions after testing (fig. 4.35). This highlights the close relationship between ceramic friability and mechanical performance.

Recoil measurements also correlate well with the established relationship between ceramic modulus or self-stiffening and the dust weight fraction produced during compression (fig. 4.26). Within the groups of varied porosity, sintering temperature and particle size, the stiffest configuration produced the highest recoil and the most friable configuration the lowest recoil. The ratio between maximum and minimum recoil within these groups was largest for porosity, second largest for sintering temperature and the lowest for particle size, an observation in perfect correlation with the measurements of modulus, modulus increase and dust weight fraction made before. High porosity as the most influential property caused the lowest recoil overall. This shows that high modulus ceramics are more elastic than friable ceramics where elastically irrecoverable particle crushing is the dominant mode of deformation.

Despite the significant differences in modulus and particle breakage observed for the various ceramic configurations, relaxation was qualitatively identical to bone and quantitatively nearly the same for all ceramics tested (fig. 4.24, 4.31 and table 4.4). Nearly all differences between the averages were statistically not significant. Relaxation must be governed by a fundamental property of HA/TCP ceramics which is unaffected by porosity, sintering temperature, chemical composition and size. The absence of a viscoelastic organic phase, which is present in bone grafts and influences relaxation, is one constant factor.

4.5.3 Discussion - bone graft and ceramic mixes

Bone grafts and ceramic graft extenders have very different mechanical properties and combining them in bone plus ceramic extender graft mixes resulted in a qualitative and quantitative combination of the properties identified for the pure phases (fig. 4.38 and 4.39). The exponential stress-strain relationship of pure bone grafts and the linear stress-strain correlation with its superimposed saw-tooth profile due to particle crushing of the ceramics are combined. With a rising ceramic content the exponent of the stress-strain curves measured for different mixes decreased while the intensity of superimposed stress peaks and drops increased. The properties of the bone and ceramic phase combine in such a way that the influence of the bone graft was disproportionately stronger as the stress-strain curves of graft mixes lay significantly closer to pure bone than ceramic.

The explanation follows from the fact that the hard and friable pure ceramics contain no viscoelastic organic material at all while the bone grafts do contain large quantities thereof. When adding even just small amounts of bone and thus organic phase to the stiff and hard ceramics, the relative strain increase is immense while at the same time particle fractures are

reduced by smoothening load transfer. Consequently, the modulus drops significantly while sudden particle fractures causing the saw-tooth profile are reduced. As ceramic granules added to a pure bone graft work in a similar way to the fragments of trabecular bone contained within bone originally, a stiffness increase for bone grafts can be expected when small ceramic volume fractions are added.

The gradual combination of properties from bone and ceramic in a graft mix and the dominant role of the bone graft is also reflected in the recoil measurements (fig. 4.42). This observation further supports the analysis that bone/ceramic graft mixes sustain bone-like characteristic properties while being structurally enhanced by the ceramics. Even for high levels of ceramics in a graft mix, the influence of small amounts of bone is strong.

When pre-compressed b/c mixes were re-loaded towards higher compression forces, the moduli increased more as the bone content increased. As a result, the stiffness values during the quasi-linear 500-1000N loading phase approached each other by so much that the difference between the 2:1 and 1:2 b/c mixes were not significant anymore. This is the result of previously described properties typical for the pure phases. While the initially exponentially rising stress-strain curves of bone grafts causes moduli to increase towards higher loads, stiffness of hard ceramic grafts with their quasi-linear stress-strain response remained nearly constant. Thus, in a bone graft mix, the modulus increase is higher, the higher the bone content.

At high loads, when high strains have compressed much of the organic phase of the bone grafts and the trabecular bone chips increasingly come into contact with each other, the load bearing capacity of a bone graft becomes progressively affected by the mechanical performance of its trabecular mineral phase. The trabecular mineral bone is mimicked by the chemically related granular HA/TCP ceramic used here as a bone graft extender and thus it can be understood why towards higher loads and strains pre-compressed bone/ceramic mixes and their constituents approach each other's stiffness.

This stiffness assimilation is aided by the geometrical set-up of the experiment where radial deformation is inhibited and thus a potential failure of the materials as a result of excessive lateral strain is subdued. In theory, any material well constrained during compression would exhibit a high and increasing stiffness once a certain strain is reached. This way properties of materials otherwise different in performance would assimilate. In the clinical situation bone grafts are also entrapped between the cement coated stem, the endosteal surface of the medullary canal and the proximal cement layer.

Investigating the relaxation behaviour of bone plus ceramic graft mixes confirms previously described analysis of the strong characteristic role of the bone phase in a b/c mix. For all graft mixes relaxation is significantly closer to the values recorded for pure bone (<11%) than for pure ceramic (>43%, fig. 4.41 and table 4.5) and comparison amongst the graft mixes reveals such small differences that in the case of relaxation no statistically significant difference was identified. In the pure ceramic materials the viscoelastic organic phase is completely absent and when added into a bone/ceramic, it mix exhibits a particularly intense effect on the relaxation behaviour. Table 4.7 summarises essential discussion points.

- **BONE**

- Bone is a multiphase material with properties defined by its phases: hard trabecular bone plus viscoelastic organic and liquid component \Rightarrow exponential stress-strain response.
- Graft stiffness only affected by bone mill, not affected by other treatments \Rightarrow Stiffness affected by the quantity and condition of bone mineral phase not organic.
- Relaxation similar for most treatments \Rightarrow similar quantities of organic tissue present.
- Relaxation of ovine graft affected by washing & drying and fixation \Rightarrow more organic tissue present.
- Properties of Norwich milled fixed ovine equal to Howex milled human graft, bovine xenograft different.
- Human bone graft more variable than xenografts due to sourcing differences.
- Howex superior to Norwich mill (stiffer, fully enclosed, hook-like blades with good spacing).

- **CERAMICS**

- Displacement is the result of granular fracture, void-filling, re-arrangement.
- Frequent granule fractures \Rightarrow Linear stress-strain results with superimposed saw-tooth profile and high standard deviation of moduli despite controlled manufacture.

Effect of parameters

- Porosity with highest effect \Rightarrow stress-concentrations in granules.
- Sintering temperature \Rightarrow phase changes and crystallinity.
- Size \Rightarrow packing and load transfer in tightly constrained environment.
- Composition with no effect \Rightarrow phase changes assimilate materials, other effects dominate or obscure.
- Post-compression dust fraction correlates with above parameter effects, friability rules properties.
- Hard ceramics have some elasticity, deformation of friable ceramics irrecoverable, crushing only.
- Property assimilation during re-compression and high stress loading \Rightarrow self-stiffening effect by increasing packing efficiency (less voids) and reducing porosity.
- Relaxation the qualitatively identical to bone and the same for all ceramics \Rightarrow no viscoelastic phase present in all ceramics.

- **BONE/CERAMIC MIXES**

- Influence of bone grafts is dominant \Rightarrow even small amounts of organic material increase strain significantly and reduce fractures of brittle ceramics.
- Assimilation towards higher stresses \Rightarrow load transfer becomes dominated by mineral phase and ceramic granules.
- Constrained compression could assimilate all graft materials eventually.

Table 4.7: Summary of discussion points after die-plunger compression testing.

4.6 Conclusions

• Conclusions - human bone graft

Human morsellised bone grafts can have different mechanical properties depending on their preparation, sterilisation and storage applied prior to clinical use. Thus in surgical impaction grafting a standard graft preparation protocol must be employed to ensure most consistent results. Also in scientific publications, authors should give accurate detail about graft production from donor to implantation in order to allow comparability of results.

Bone grafting processes which influence the size and morphology of the trabecular bone such as bone mill type and blade size can change the stiffness and possibly the stability potential of the bone graft. It can also reduce the variability of morsellised bone chips. The Howex bone mill offers a more solid design and a superior blade to the Norwich bone mill and should be the preferred alternative to morsellise graft for stable and less variable impaction grafting procedures. For maximising stiffness and stability further, stiff and strong cortical bone fragments should be left or intentionally included in the graft.

Other graft preparation, sterilisation and storage procedures tested did not significantly affect stiffness, so that no detrimental effect on graft stability must be expected. This conclusion is also valid for γ -irradiation at the typical bone bank doses of 2.5 MRad and 5MRad, often legally required for sterilisation in clinical application. Also washing and drying the graft, a procedure that has been reported to offer superior stability in clinical impaction grafting, did not produce increased bone graft stiffness to elucidate such an improvement. An explanation will follow below. Also multiple freeze/thaw cycles which might appear in the clinical storage and preparation chain do not negatively affect stiffness and thus the stability potential of bone grafts. This means that preparation of large graft quantities which helps levelling out variability of individual femoral heads and raises convenience during *in-vitro* experimental studies is a viable option without potential effects on stability. With regards to stiffness, this can also be claimed for formalin fixation of human bone, a procedure possibly required in certain low-level biohazard laboratories.

Graft relaxation and recoil could affect the sensory feedback of the surgeon during manual impaction, an important subjective measure for the personal assessment whether sufficient impaction is achieved. Some graft preparation, sterilisation and storage methods did slightly affect the relaxation and recoil behaviour of the human bone graft. However, the measured differences were so small and the standard deviations within the sample groups so large that

most comparisons were not statistically significant. No trend was identifiable. Consequently, no effect on the sensory feedback to the surgeon during impaction grafting must be expected.

The wetness or liquid content of a human bone graft in the form of blood, water or other fluids showed strong effects on the mechanical performance when fluid escape was suppressed during compression. Reaction forces ramped up steeply without much strain so that no further graft compaction was achieved. This was the case when the plunger was non-porous when strain rates were too high to allow adequate fluid escape. A similar condition is prevalent during clinical impaction when fresh and thus bloody graft is impacted into the medullary canal. The distal plug seals fluid escape distally and the endosteal surfaces of the medullary have insignificant permeability to discharge fluids squeezed out during impaction. The medullary canal even provides additional blood at pressure into the compaction space. The impactors have flat solid ends and seal off most of the proximal fluid escape route.

From this analysis it can be concluded that during clinical impaction grafting a lot of impaction energy is wasted for squeezing out fluids from the graft instead of compacting and thus stabilising it. The hammer blows are dampened viscoelastically so that peak forces acting into the graft are reduced and compaction intensity is sacrificed. When bone graft is washed and dried prior to impaction, the hammer energy will be delivered more effectively and with higher peak forces. Under the assumption of equal hammer energies delivered, the graft will be compacted to a higher degree and a better stability could be achieved. This should be the dominating effect why surgeons have observed better clinical stability in patients when washed and dried grafts were used. In order to optimise stability, surgeons should wash and dry or at least dry their graft prior to impaction. Permanent and effective fluid removal during impaction might also aid stability. The use of freeze-dried graft can be recommended as well.

Anticipating one item of conclusions closely examined later, the use of a ceramic bone extender in a graft mix could also solve or reduce the wetness and fluid escape problem. Firstly, dry ceramic granules reduce the liquid content by replacing a fraction of wet bone graft and secondly, depending on porosity, ceramics can soak up fluids without releasing them during impaction.

Conclusions - xenografts

Fresh morsellised xenografts are not suited for clinical impaction grafting due to uncontrollable risks of infection and rejection. Xenografts which have been used for impaction and other kinds of bone grafting are sterilised or demineralised in such intense ways that they have no resemblance to fresh morsellised graft but form a class of bone grafts

of their own. Fresh and treated xenografts were investigated in this study as potential experimental bone grafts for *in-vitro* testing of the impaction grafting procedure, implants, tools or new bone graft extenders. *In-vitro* mechanical tests can require large quantities of bone grafts with consistent quality and this is not available from human donors for ethical, supply or cost reasons.

Ovine bone grafts registered stiffness and relaxation values in the same range as the differently prepared human bone grafts. In particular stiffness comparisons between ovine and the Howex milled human grafts did not reveal statistically significant differences. With regards to relaxation, fresh ovine graft and washed and dried ovine graft were most similar to human bone whereas the relaxation of fixed ovine graft was significantly different to all human grafts. This indicates a higher organic fraction present in the ovine grafts which is affected during the sterilisation process. However, this relaxation difference measured less than 4%, a non-perceptible value during surgical impaction grafting. Considering the statistically indistinguishable compression moduli of human and ovine graft and bearing in mind the low variability of graft properties, ovine bone is a highly suitable experimental graft for *in-vitro* testing. Even if ovine graft tends to have slightly higher stiffness and slightly lower relaxation and recoil values than the human reference, during mechanical testing of synthetic bone alternatives in graft mixes, this effect would conservatively raise demands for improved stability of such materials.

The wetness of ovine graft appeared to be less than human graft. During compaction at high strain rates, like those present during clinical impaction or experimental compaction with hammer blows, the lower blood and fluid content of ovine bone could lead to denser graft compaction. This could enhance the stability of ovine against human graft. However, if human bone is dried, energy conversion from impaction blows to graft compaction should be equally efficient, so that ovine graft remains a valid xenograft for *in-vitro* mechanical testing.

Morsellised bovine bone cannot be recommended as an experimental graft with the same confidence as ovine graft. Relaxation of bovine and human graft was similar and differences not significant in some cases. However, the compression moduli of bovine bone measured during initial compression and during secondary compression were the highest of all bone grafts. The moduli were up to 50% more than for human graft and differences were significant in all cases. This is the consequence of bovine bone having a much denser and thus stronger trabecular structure which is easily visible to the human eye. The density and structure of trabecular bovine bone compares to the cancellous bone from equine femoral and

humeral heads also assessed for comparison. Like bovine graft, equine bone also cannot be recommended as a replacement for human bone during *in-vitro* testing.

Conclusions - ceramics

The stress-strain response of all granular HA/TCP ceramics tested as synthetic bone graft substitutes was qualitatively and quantitatively entirely different from human and xenograft bone. This correlates with the completely different appearance and handling properties, both relevant for mental acceptance by clinicians and for surgical application. Aggregates of pure ceramic particles can be up to seven times stiffer than morsellised bone. During compression, ceramic displacement is less the result of elastic or plastic deformation as with bone, but more the consequence of crushing, void filling and the granular re-arrangement of the brittle and friable ceramic particles. This is also the reason why relaxation of ceramics is much lower than for bone. Granular ceramics do not mimic bone properties at all in their attempt to substitute bone. Thus, in pure form ceramic granules are not suited to replace morsellised bone in impaction grafting completely. However, they are well suited as bone graft extenders in bone/ceramic mixes as their properties can improve the mechanical properties.

Porosity was by far the single most influential parameter on the mechanical properties of the granular ceramic bone substitutes. High porosity introduces large numbers of intra-granular stress concentrations triggering crack formation under load. Highly porous granules break up into many small and dust-like particles causing high deformation and low stiffness moduli. If ceramic porosity is maximised for optimum osteoconductive properties, the friability of such a porous ceramic can be so high that the compression modulus is lower than that of bone rendering it unsuitable for bone replacement in load bearing applications such as impaction grafting. Vigorous impaction blows and *in-vivo* loading would not compact and stabilise the graft but only convert it into dust. Crushed to powder, the original porosity is lost and with it the osteoconductive advantage aimed for.

As ceramic porosity shows, maximising graft stability and osteoconductivity results in a conflict between mechanical and biological requirements. Bone apposition, vascularisation, resorption and remodelling is a function of porosity level and benefits from highly interconnected macropores throughout the granules. Maximising these parameters for the biological advantage will create ceramic graft substitutes less stiff and stable than the bone reference. In order to avoid this risk, a certain porosity level and interconnectivity must not be exceeded. From the porosity levels tested in this study, a maximum of ca. 50-60% porosity should not be exceeded and depends on pore size, pore distribution and interconnectivity. However, the strong correlation between mechanical stiffness and porosity might dilute to a

degree when the ceramic is used in a bone/extender graft mix. Then ceramic cracking triggered by direct contact of brittle and friable granules becomes partially subdued by the viscoelastic organic phase smoothing the load transfer through the mix.

As a viable compromise between biological and mechanical demands, the ceramic granules could be designed to concentrate porosity on the outer surface to accelerate bone on-growth and improve interface strength while retaining a less porous core securing sufficient stability. Alternatively, other ceramic parameters such as sintering temperature, duration or chemical composition could be optimised towards higher stability to compensate stability lost by porosity maximised for biological benefit, marketing purposes and clinical acceptance. However, apart from potentially stabilising a porous ceramic, these parameters could affect pore formation during sintering or the biological response by, for instance, changing the resorption rate.

Second to porosity, sintering temperature had the strongest influence on the mechanical properties of the ceramic graft. Too low temperatures led to insufficient sintering of the HA and TCP powders and resulted in highly friable granules which were not only less stiff but also produced high volume fractions of dust under loading. Similar to highly porous ceramics, the friable low temperature ceramics lose their osteoconductively active porosity when broken down into dust-like particles with diameters below the size of pores biologically required. In addition, friable ceramics producing high weight fractions of dust create particles of potentially cytotoxic dimensions similar to the wear debris of the ball/cup surface. With those particles being generated close to the region where aseptic loosening of the stem can be triggered by migrating polyethylene debris, the risk of giving rise to osteolysis by ceramic debris must be considered and minimised when HA/TCP graft extenders are sintered.

Raising the sintering temperature increased stiffness and significantly reduced dust production under loading. This trend continued with decreasing intensity when the sintering temperature was raised further towards degradation point. Sintering at high temperatures and for long periods of time causes phase changes in the composite ceramic which can influence the resorption rate in a biological environment. Nevertheless sintering temperature should be high to maximise stiffness in order to allow maximum porosity levels without sacrificing stability and in order to minimise potentially cytotoxic dust production.

Small ceramic granules produced higher stiffness values than the large particles due to packing and load transfer advantages in the geometrically constrained testing environment which mimics the dimensional relationships of the medullary cavity, stem and graft in clinical

impaction grafting. However, the issue of ideal granule size cannot be safely concluded from this observation because the ceramic grafts tested in this study should not be used in pure form like during the die-plunger test, but only as graft extenders in a mix with bone. Here, a wide particle size range combines and influences packing and load transfer. Nevertheless, the packing and load transfer advantages of the small granules could persist and even weigh stronger in a bone/ceramic mix. Particle size analysis of morsellised bone graft^[224] suggests that it contains insufficient quantities of small particles to form the so-called Fuller's size distribution curve, a theoretical packing optimum derived for soils in civil engineering. However, soil mechanics theory might not be fully applicable here as it is derived on the premise of unlimited extension of the particulate aggregate, an idealised situation not present in impaction grafting. Nevertheless, in a b/c mix small particles would have the advantage that preparing a homogenous mix becomes easier and that it could be charged more easily without segregation.

Reversing the chemical composition of the HA/TCP composite did not result in significantly different compression moduli. Considering the different mechanical properties of the pure HA and TCP phases in bulk, this is a surprise. It might be the result of complex phase changes during sintering or it might be the effect of the granular form and the constrained test conditions which override modulus differences detectable in bulk samples. As such differences would become diluted even further in a bone/ceramic mix, the chemical composition seems to be a variable which can be changed as desired without sacrificing stability. Thus it could be used to optimise resorption, manufacturing, marketing or cost.

Relaxation was the same for all ceramic configurations. As relaxation of a graft might influence surgical assessment of impaction quality different ceramic graft extenders from the tested range do not alter this feedback so that surgeons would not need to adapt if the formulation changed.

Conclusions - bone/ceramic mixes

Bone/ceramic mixes qualitatively and quantitatively combine properties of their constituents as a function of mixing ratios. As a result, bone grafts mixed with the standard HA/TCP ceramic offered significantly increased stiffness for all mixing ratios while retaining the exponential stress-strain response typical for bone during initial low force compression and the quasi-linear stress-strain response characteristic during high force compression. In clinical practice this means that mixing a ceramic extender of reproducible properties into the morsellised bone allows the controlled manipulation of overall graft properties as a function of mixing ratio.

For all mixing ratios, including the high ceramic content 1:2 b/c mix, compression moduli and the qualitative stress-strain responses were much closer to pure bone than to the pure ceramic. The stiffness differences between the various mixing ratios were relatively small. The same applies for graft recoil, an important characteristic relevant for intra-operative feedback from the impaction process.

At higher compression forces, the modulus differences between the mixes themselves and to pure bone nearly disappeared. Differences in relaxation were even not statistically significant for the mixes. Relaxation averages were also much closer to pure bone than to ceramic. In clinical application this means that even small amounts of ceramic granules added to the bone can mechanically enhance the graft while the qualitative characteristics of pure bone grafts are well retained even for high ceramic ratios. A surgeon should be able to handle and impact such a graft mix in much the same way as he is familiar with from using pure bone chips. A surgeon should also continue to rely on his sensory feedback from the impaction process. As differences in stiffness, relaxation and recoil are small between graft mixes, preparing such mixes in theatre is a process highly tolerant to variations of the bone/ceramic ratio. Potential mixing errors or phase segregation during charging would not have detrimental effects on stability against pure bone. As most ceramic graft extenders enhance the stiffness of a bone graft, raising the mixing ratio by mistake or process tolerances can only enhance stability.

Compressing morsellised bone, granular ceramic and different mixes thereof into a small constrained volume leads to an assimilation of stiffness and stability potential when samples are compressed repetitively or when compression loads increase. This suggests that intense impaction and secure proximal containment are the most crucial surgical process variables to control and secure. In consequence, almost any bone graft, synthetic extender or mix thereof could provide sufficient stability once good impaction and proximal containment are secured. All configurations of the HA/TCP ceramic bone substitutes promise to be highly suitable for extending bone graft in clinical application saving human bone and improving stability. A summary of essential conclusions is listed in table 4.8.

- **HUMAN BONE**
 - Graft properties can be affected by preparation, storage, sterilisation \Rightarrow standard clinical protocol and full disclosure in publications required.
 - Procedures affecting size, morphology or fraction of trabecular chips can increase stiffness and thus stability in impaction grafting \Rightarrow cortical fragments are beneficial.
 - No stiffness and thus no stability lost for irradiation and multiple freeze/thaw cycles \Rightarrow clinical and experimental grafting can be safer, easier and less variable.
 - Relaxation and recoil was slightly affected by some methods but not significantly for most \Rightarrow no negative effect on sensory impaction feedback.
 - Blood dampens hammer blows \Rightarrow compaction intensity and stability is sacrificed. Beneficial: Less blood through washing & drying, good intra-operative blood removal, use of freeze dried grafts, use of ceramic extenders retaining blood, new impactor designs.
- **XENOGRAFTS**
 - Fixed ovine (standard experimental graft) and Howex milled human bone (common clinical graft) not significantly different \Rightarrow excellent experimental *in-vitro* graft.
 - Bovine bone up to 50% stiffer than human bone. Less suitability as experimental graft.
- **CERAMICS**
 - Completely different to bone qualitatively and quantitatively \Rightarrow function not based on bone mimicry.
 - Improve mechanical properties in a customisable b/c mix \Rightarrow suitable bone extender for load bearing applications.
 - Different appearance and handling \Rightarrow problems with mental acceptance and surgical handling.
 - Porosity highly critical for stability \Rightarrow Trade-off between mechanical and biological demands.
 - Maximum recommended porosity ca. 50-60%. Higher porosity and osteoconductivity aimed for will be lost due to dusting during impaction and loading.
 - Low T_{Sint} –ceramics are friable like highly porous grafts \Rightarrow high dust levels during compaction \Rightarrow cytotoxic wear debris.
 - Ideal ceramic size difficult to conclude from die-plunger tests.
 - Small granules were the stiffest and seem advantageous \Rightarrow easy mixing, low segregation during handling.
 - Composition without effect \Rightarrow can be altered to optimise resorption, manufacture, marketing cost.
 - Relaxation identical for all ceramics \Rightarrow no difference in surgical impaction feedback.
- **MIXES**
 - Mixes combine the distinctively different properties of bone and ceramic \Rightarrow b/c mixes can be manipulated as desired by adapting the b/c ratio.
 - Differences between mixes are low and disappear at high loads \Rightarrow Clinical mixing errors or phase segregation during charging is not critical.
 - Differences between all grafts assimilate during multiple re-loading and towards higher loads \Rightarrow when dense compression and stiff containment is secured, any graft can provide stability.

Table 4.8: Summary of conclusion drawn from die-plunger compression testing.

